

Multiple Pathways for Dinitrogen Activation during the Reduction of an Fe Bis(iminepyridine) Complex

Jennifer Scott,[†] Indu Vidyaratne,[†] Ilia Korobkov,[†] Sandro Gambarotta,^{*†} and Peter H. M. Budzelaar^{*‡}

Department of Chemistry, University of Ottawa, Ottawa, ON K1N 6N5, Canada, and Department of Chemistry, University of Manitoba, Winnipeg, MB R3T 2N2, Canada

Received August 20, 2007

Reduction of the bis(iminopyridine) FeCl₂ complex {2,6-[2,6-(Pr)₂PhN=C(CH₃)₂(C₅H₃N)]₂}FeCl₂ using NaH has led to the formation of a surprising variety of structures depending on the amount of reductant. Some of the species reported in this work were isolated from the same reaction mixture, and their structures suggest the presence of multiple pathways for dinitrogen activation. The reaction with 3 equiv of NaH afforded {2-[2,6-(Pr)₂PhN=C(CH₃)]-6-[2,6-(Pr)₂PhN-C=CH₂](C₅H₃N)}Fe(μ,η²-N₂)Na (THF) (**1**) containing one N₂ unit terminally bound to Fe and side-on attached to the Na atom. In the process, one of the two imine methyl groups has been deprotonated, transforming the neutral ligand into the corresponding monoanionic version. When 4 equiv were employed, two other dinitrogen complexes {2-[2,6-(Pr)₂PhN=C(CH₃)]-6-[2,6-(Pr)₂PhN-C=CH₂](C₅H₃N)}Fe(μ-N₂)Na(Et₂O)₃ (**2**) and {2,6-[2,6-(Pr)₂PhN=C(CH₃)₂(C₅H₃N)]₂}Fe(μ-N₂)Na[Na(THF)₂] (**3**) were obtained from the same reaction mixture. Complex **2** is chemically equivalent to **1**, the different degree of solvation of the alkali cation being the factor apparently responsible for the σ-bonding mode of ligation of the N₂ unit to Na, versus the π-bonding mode featured in **1**. In complex **3**, the ligand remains neutral but a larger extent of reduction has been obtained, as indicated by the presence of two Na atoms in the structure. A further increase in the amount of reductant (12 equiv) afforded a mixture of {2-[2,6-(Pr)₂PhN=C(CH₃)]-6-[2,6-(Pr)₂PhN-C=CH₂](C₅H₃N)}Fe-N₂ (**4**) and [{2,6-[2,6-(Pr)₂PhN=C(CH₃)₂(C₅H₃N)]₂-Fe-N₂]₂(μ-Na) [Na(THF)₂]₂ (**5**) which were isolated by fractional crystallization. Complex **4**, also containing a terminally bonded N₂ unit and a deprotonated anionic ligand bearing no Na cations, appears to be the precursor of **1**. The apparent contradiction that excess NaH is required for its successful isolation (**4** is the least reduced complex of this series) is most likely explained by the formation of the partner product **5**, which may tentatively be regarded as the result of aggregation between **1** and **3** (with the ligand system in its neutral form). Finally, reduction carried out in the presence of additional free ligand afforded {2,6-[2,6-(Pr)₂PhN=C(CH₃)₂(C₅H₃N)]₂}Fe(η¹-N₂){2,6-[2,6-(Pr)₂PhN=C(CH₃)₂(NC₅H₂)]₂}[Na(THF)₂] (**6**) and {2,6-[2,6-(Pr)₂PhN=C(CH₃)₂(C₅H₃N)]₂}Fe{2,6-[2,6-(Pr)₂PhN=C(CH₃)₂(NC₅H₂)]₂}[Na(THF)₂] (**7**). In both species, the Fe metal is bonded to the pyridine ring para position of an additional (L)Na unit. Complex **6** chemically differs from **7** (the major component) only for the presence of an end-on coordinated N₂.

Introduction

Dinitrogen activation/fixation has been observed with almost all of the metals and f-block elements, with particular recurrence among strongly reducing, low-valent, early metal systems.^{1–3} In fact, the large volume and variety of trans-

formations involving early metal dinitrogen complexes, including N–N triple bond cleavage,^{1,2,3b–d,i–m,o,q} partial reduction followed by elemental modifications,^{3a,e–g,p,r–v} or incorporation into the ligand system,³ⁿ has made early metal complexes the most popular targets for these studies, and several recent reviews detail the latest developments in this area.⁴ As a matter of fact, dinitrogen chemistry involving late transition metals remains substantially less developed, possibly as a result of the rather general lability of late metal dinitrogen complexes.^{4–8} This is in spite of the fact that Fe is a key element in nitrogenase enzymes.⁹ Furthermore, it is

* To whom correspondence should be addressed. E-mail: sgambaro@science.uottawa.ca (S.A.), budzelaar@cc.umanitoba.ca (P.H.M.B.).

[†] University of Ottawa.

[‡] University of Manitoba.

(1) (a) Yandulov, D. V.; Schrock, R. R. *Science* **2003**, *301*, 76. (b) Schrock, R. R. *Acc. Chem. Res.* **2005**, *38*, 955.

now established that nitrogenase initially forms a dinitrogen complex, possibly *weakly* bound, which then undergoes stepwise reduction toward ammonia via multiple association–dissociation with the Fe–protein residue.¹⁰ What makes nitrogenase so unique is the ability to perform electron-

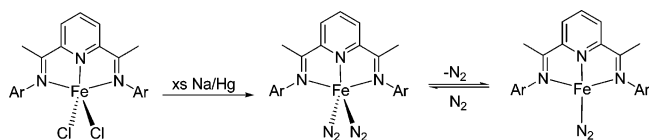
coupled proton transfer¹¹ as a key step in the catalytic cycle, having no parallel in any “man-made” fixation system.

Dinitrogen complexes of Fe have been observed on several occasions and in most cases display minimal activation of the N–N triple bond.^{5–8} Especially intriguing from this point of view has been the observation by Smith et al. of an end-on bridging dinitrogen Fe complex which, upon subsequent reduction, undergoes significant electron transfer to the N₂ unit accompanied by only a minor elongation of the N–N distance.⁶ This strange behavior also has a parallel in the chemistry of low-valent samarium, where further reduction of the coordinated N₂ unit was reported to result in a *shortening* of the N–N triple bond prior to cleavage.¹² Although changes in N–N bond length determined by X-ray diffraction need to be treated with caution, to date, reduction to an N=N double bond is the greatest amount of activation witnessed for an Fe-bound N₂ moiety.⁶ Yet, Betley and Peters have demonstrated the possibility of generating a bridging triple-bond Fe–dinitrogen complex through the six-electron redox reaction between two Fe^{IV}=N complexes.^{7a} Thus, by microscopic reversibility, the reverse reaction involving the six-electron cleavage of a bridging dinitrogen ligand toward two nitrido moieties should be kinetically possible.

The appropriate choice of the ligand system is, as always, central to finding the desired transformation. The observation that reduction of the dinitrogen unit in both the Fe⁶ and Sm¹² systems does not parallel an elongation of the N–N bond distances suggested to us that the use of a ligand system which may work as an electronically flexible π -acceptor could be beneficial to the success of dinitrogen activation/fixation. It was hoped that if some of the electrons could be stored in electronically flexible ancillary ligands, a sufficient number of electrons could potentially be accumulated in the complex to eventually effect cleavage of the N–N bond. In turn, this could overcome the problem of the high energy of some of the critical intermediates. The aryl bis(iminepyridine) ligand has proven to be ideally suited for this purpose, having produced complexes where the metal is present in very unusually low *formal* oxidation states.^{8,13–19} Even more remarkable is the fact that although the reduction occurs at

- (2) Pool, J. A.; Lobkovsky, E.; Chirik, P. J. *Nature* **2004**, *427*, 527.
- (3) (a) Berno, P.; Gambarotta, S. *Angew. Chem., Int. Ed.* **1995**, *34*, 822. (b) Laplaza, C. E.; Cummins, C. C. *Science* **1995**, *268*, 861. (c) Cui, Q.; Musaev, D. G.; Svensson, M.; Sieber, S.; Morokuma, K. *J. Am. Chem. Soc.* **1995**, *117*, 12366. (d) Laplaza, C. E.; Johnson, M. J. A.; Peters, J. C.; Odom, A. L.; Kim, E.; Cummins, C. C.; George, G. N.; Pickering, I. J. *J. Am. Chem. Soc.* **1996**, *118*, 8623. (e) Zanotti-Gerosa, A.; Solari, E.; Giannini, L.; Floriani, C.; Cheisi-Villa, A.; Rizzoli, C. *J. Am. Chem. Soc.* **1998**, *120*, 437. (f) Ishino, H.; Tokunaga, S.; Seino, H.; Ishii, Y.; Hidai, M. *Inorg. Chem.* **1999**, *38*, 2489. (g) Peters, J. C.; Cherry, J. P. F.; Thomas, J. C.; Baraldo, L.; Mendiola, D. J.; Davis, W. M.; Cummins, C. C. *J. Am. Chem. Soc.* **1999**, *121*, 10053. (h) Tsai, Y. C.; Johnson, M. J. A.; Mendiola, D. J.; Cummins, C. C.; Klooster, W. T.; Koetzle, J. F. *J. Am. Chem. Soc.* **1999**, *121*, 10426. (i) Clentsmith, G. K. B.; Bates, V. M. E.; Hitchcock, P. B.; Cloke, F. G. N. *J. Am. Chem. Soc.* **1999**, *121*, 10444. (j) Caselli, A.; Solari, E.; Scopelliti, R.; Floriani, C.; Re, N.; Rizzoli, C.; Chiesi-Villa, A. *J. Am. Chem. Soc.* **2000**, *122*, 3652. (k) Mendiola, D. J.; Meyer, K.; Cherry, J. P. F.; Baker, T. A.; Cummins, C. C. *Organometallics* **2000**, *19*, 1622. (l) Solari, E.; Silva, C. D.; Iacono, B.; Heschentruck, J.; Rizzoli, C.; Scopelliti, R.; Floriani, C. *Angew. Chem., Int. Ed.* **2001**, *40*, 3907. (m) Yandulov, V.; Schrock, R. R. *J. Am. Chem. Soc.* **2002**, *124*, 6252. (n) Fryzuk, M. D.; Kozak, C. M.; Bowdridge, M. R.; Patrick, B. O.; Rettig, S. J. *J. Am. Chem. Soc.* **2002**, *124*, 8389. (o) Kawaguchi, H.; Matsuo, T. *Angew. Chem., Int. Ed.* **2002**, *41*, 2792. (p) Fryzuk, M. D.; MacKay, B. A.; Johnson, S. A.; Patrick, B. O. *Angew. Chem., Int. Ed.* **2002**, *41*, 3709. (q) Tsai, Y.-C.; Cummins, C. C. *Inorg. Chim. Acta* **2003**, *345*, 63. (r) Fryzuk, M. D.; MacKay, B. A.; Patrick, B. O. *J. Am. Chem. Soc.* **2003**, *125*, 3234. (s) Shaver, M. P.; Fryzuk, M. D. *Adv. Synth. Catal.* **2003**, *345*, 1061. (t) Mizobe, Y.; Ishii, Y.; Hidai, M. *Coord. Chem. Rev.* **1995**, *139*, 281. (u) Bernskoetter, W. H.; Lobkovsky, E.; Chirik, P. J. *Angew. Chem., Int. Ed.* **2007**, *46*, 2858. (v) Morello, L.; Love, J. B.; Patrick, B. O.; Fryzuk, M. D. *J. Am. Chem. Soc.* **2004**, *126*, 9480.
- (4) For recent reviews see: (a) MacLachlan, E. A.; Fryzuk, M. D. *Organometallics* **2006**, *25*, 1530. (b) Gambarotta, S. *J. Organomet. Chem.* **1995**, *500*, 117. (c) Gambarotta, S.; Scott, J. *Angew. Chem., Int. Ed.* **2004**, *43*, 5289. (d) MacKay, B. A.; Fryzuk, M. D. *Chem. Rev.* **2004**, *104*, 385. (e) Hidai, M.; Mizobe, Y. *Chem. Rev.* **1995**, *95*, 1115. (f) Hidai, M. *Coord. Chem. Rev.* **1999**, *185–186*, 99. (g) Fryzuk, M. D.; Johnson, S. A. *Coord. Chem. Rev.* **2000**, *200–202*, 379. (h) Kozak, C. M.; Mountford, P. *Angew. Chem., Int. Ed.* **2004**, *43*, 1186. (i) Fryzuk, M. D.; Love, J. B.; Rettig, S. J.; Young, V. G. *Science* **1997**, *275*, 1445. (j) Basch, H.; Musaev, D. G.; Morokuma, K.; Fryzuk, M. D.; Love, J. B.; Seidel, W. W.; Albinati, A.; Koetzle, T. F.; Klooster, W. T.; Mason, S. A.; Eckert, J. *J. Am. Chem. Soc.* **1999**, *121*, 523. (k) Fryzuk, M. D.; Johnson, S. A.; Rettig, S. J. *J. Am. Chem. Soc.* **1998**, *120*, 11024. (l) Fryzuk, M. D.; Johnson, S. A.; Patrick, B. O.; Albinati, A.; Mason, S. A.; Koetzle, T. F. *J. Am. Chem. Soc.* **2001**, *123*, 3960.
- (5) (a) Hills, A.; Hughes, D. L.; Jimenez-Tenorio, M.; Leigh, G. J. *J. Organomet. Chem.* **1990**, *391*, C41. (b) Komiyama, S.; Akita, M.; Yoza, A.; Kasuga, N.; Fukuoka, A.; Kai, Y. *J. Chem. Soc., Chem. Commun.* **1993**, 787. (c) Hills, A.; Hughes, D. L.; Jimenez-Tenorio, M.; Leigh, G. J. *J. Chem. Soc., Dalton Trans.* **1993**, 3041. (d) Leal, A. D.; Jimenez-Tenorio, M.; Puerta, M. C.; Valerga, P. *Organometallics* **1995**, *14*, 3839. (e) George, T. A.; Rose, D. J.; Chang, Y.; Chen, Q.; Zubieta, J. *Inorg. Chem.* **1995**, *34*, 1295. (f) Hirano, M.; Akita, M.; Morikita, T.; Kubo, H.; Fukuoka, A.; Komiyama, S. *J. Chem. Soc., Dalton Trans.* **1997**, 3453. (g) Wiesler, B. E.; Lehnert, N.; Tuzcek, F.; Neuhäuser, J.; Tremel, W. *Angew. Chem., Int. Ed.* **1998**, *37*, 815. (h) Berke, H.; Bankhardt, W.; Huttner, G.; von Seyerl, J.; Zsolnai, L. *Chem. Ber.* **1981**, *114*, 2754. (i) Kandler, H.; Gauss, C.; Bidell, W.; Rosenberger, S.; Bürgi, T.; Eremenko, I. L.; Veghini, D.; Orama, O.; Burger, P.; Berke, H. *Chem. Eur. J.* **1995**, *1*, 541. (j) Danopoulos, A. A.; Wright, J. A.; Motherwell, W. B. *Chem. Commun.* **2005**, 784. (k) Van Der Sluys, L. S.; Eckert, J.; Eisenstein, O.; Hall, J. H.; Huffman, J. C.; Jackson, S. A.; Koetzle, T. F.; Kubas, G. J.; Vergamini, P. J.; Caulton, K. G. *J. Am. Chem. Soc.* **1990**, *112*, 4831. (l) Ghilardi, C. A.; Midollini, S.; Sacconi, L.; Stoppioni, P. *J. Organomet. Chem.* **1981**, *205*, 193.
- (6) Smith, J. M.; Lachicotte, R. J.; Pittard, K. A.; Cundari, T. R.; Lukat-Rodgers, G.; Rodgers, K. R.; Holland, P. L. *J. Am. Chem. Soc.* **2001**, *123*, 9222.
- (7) (a) Betley, T. A.; Peters, J. C. *J. Am. Chem. Soc.* **2004**, *126*, 6252. (b) Mankad, N. P.; Whited, M. T.; Peters, J. C. *Angew. Chem., Int. Ed.* **2007**, *46*, 5768. (c) Betley, T. A.; Peters, J. C. *J. Am. Chem. Soc.* **2003**, *125*, 10782.
- (8) Bart, S. C.; Lobkovsky, E.; Chirik, P. J. *J. Am. Chem. Soc.* **2004**, *126*, 13794.
- (9) (a) Leigh, G. J. *Acc. Chem. Res.* **1992**, *25*, 177. (b) Howard, J. B.; Rees, D. C. *Chem. Rev.* **1996**, *96*, 2965. (c) Burgess, B. K.; Lowe, D. J. *J. Chem. Rev.* **1996**, *96*, 2983. (d) Burgess, B. K. *Chem. Rev.* **1990**, *90*, 1377.
- (10) (a) Seefeldt, L. C.; Dance, I. G.; Dean, D. R. *Biochemistry* **2004**, *43*, 1401. (b) Seefeldt, L. C.; Dean, D. R. *Acc. Chem. Res.* **1997**, *30*, 260.
- (11) Lanzilotta, W. N.; Christiansen, J.; Dean, D. R.; Seefeldt, L. C. *Biochemistry* **1998**, *37*, 11376.
- (12) (a) Evans, W. J.; Ulibarri, T. A.; Ziller, J. W. *J. Am. Chem. Soc.* **1988**, *110*, 6877. (b) Guan, J.; Dubé, T.; Gambarotta, S.; Yap, G. P. A. *Organometallics* **2000**, *19*, 4820.
- (13) Vidyaratne, I.; Gambarotta, S.; Korobkov, I.; Budzelaar, P. H. M. *Inorg. Chem.* **2005**, *44*, 1187.
- (14) Bart, S. C.; Chlopek, K.; Bill, E.; Bouwkamp, M. W.; Lobkovsky, E.; Neese, F.; Wieghardt, K.; Chirik, P. J. *J. Am. Chem. Soc.* **2006**, *128*, 13901.
- (15) Vidyaratne, I.; Scott, J.; Gambarotta, S.; Budzelaar, P. H. M.; Korobkov, I. *Inorg. Chem.* **2007**, *46*, 7040.

Scheme 1



the ligand instead of at the metal center, the metal atoms still maintain the very high reactivity expected for true low-valent species. The bis(iminepyridine) ligand has been used to prepare dinitrogen complexes of vanadium,¹³ chromium,¹⁵ iron,^{8,14} and cobalt.^{20,21} In the case of Cr, it has allowed reduction, cleavage, and partial hydrogenation of N₂ as well as the trapping of an intermediate prior to cleavage.¹⁵ For Fe, Bart et al. have reported the reduction of bis(iminepyridine)–Fe^{II} complexes to mono- and bis(dinitrogen) complexes containing *formally* zero-valent iron (Scheme 1).⁸ Unlike the end-on *bridged* N₂ units in the V and Cr systems, the end-on *terminal* dinitrogen moieties of the Fe complex exhibit minimal elongation of the triple bond. Computational studies have shown that the ligand, rather than the metal center or the labile dinitrogen unit, is the recipient of the added electron density.¹⁴ The lability of the coordinated dinitrogen has enabled the use of these species for a promising variety of metal-promoted transformations.^{8,22}

Herein, we report the results of our exploration of the reduction of the bis(iminepyridine) FeCl₂ complex using NaH as a reducing agent. This particular reductant combines electron-donating capabilities with the presence of hydrogen atoms, which is desirable for the formation of critical intermediates in the transformation of N₂ to ammonia. Different from the case of chromium,¹⁵ we did not yet succeed in obtaining dinitrogen cleavage in this case. Nevertheless, the reaction has unveiled the existence of a surprising variety of dinitrogen complexes depending on the amount of reducing agent. Herein we report our findings.

Experimental Section

All operations were performed either under a nitrogen atmosphere using standard Schlenk techniques or in a purified nitrogen-filled drybox. FeCl₂(THF)_{1.5} was prepared according to a standard procedure, and the ligand 2,6-[2,6-(*i*-Pr)₂PhN=C(CH₃)₂](C₅H₃N) was

prepared according to published procedures.²³ Suspensions of metallic sodium and NaH were purchased from Aldrich, washed with hexane, and dried prior to use. Infrared spectra were recorded on a Mattson 9000 and Nicolet 750-Magna FT-IR instrument from Nujol mulls prepared in a dry box. Samples for magnetic susceptibility measurements were weighed inside a dry box equipped with an analytical balance and sealed into calibrated tubes, and the measurements were carried out at room temperature with a Gouy balance (Johnson Matthey). Magnetic moments were calculated following standard methods, and corrections for underlying diamagnetism were applied to the data. However, for these strongly reduced iron species there is always the possibility of contamination with trace amounts of metallic iron or iron hydroxides leading to unrealistically high observed susceptibilities. Therefore, the magnetic moments reported below should be treated with caution. Data for X-ray crystal structure determinations were obtained with a Bruker diffractometer equipped with a Smart CCD area detector.

Preparation of {2-[2,6-(*i*-Pr)₂PhN=C(CH₃)₂]-6-[2,6-(*i*-Pr)₂PhN=C(CH₃)₂](C₅H₃N)}Fe(μ,η²-N₂)/Na(THF) (1). A suspension of FeCl₂(THF)_{1.5} (0.15 g, 0.64 mmol) and 2,6-[2,6-(*i*-Pr)₂PhN=C(CH₃)₂](C₅H₃N) (0.306 g, 0.64 mmol) in THF (10 mL) was added to a suspension of 3.1 equiv of NaH (0.048 g, 1.98 mmol) in THF (5 mL). The color of the solution slowly changed from dark blue to dark reddish-burgundy over the period of 2 days. Stirring was continued for an additional 5 days, the solvent was evaporated in vacuo, and fresh THF was added to the dark residue. Centrifugation allowed the separation of a dark brown solution from a mass of dark precipitates. Crystals of **1** were obtained from the mother liquor upon standing for a few days at room temperature (0.089 g, 0.13 mmol, 21% yield). IR (Nujol mull, cm⁻¹): 1912 (s), 1630 (m), 1573 (s), 1513 (w), 1463 (s), 1378 (s), 1366 (w), 1340 (w), 1324 (m), 1242 (m), 1211 (w), 1195 (w), 1099 (w), 1084 (w), 1056 (m), 1021 (w), 998 (m), 959 (w), 936 (w), 881 (m), 805 (s), 767 (w), 759 (w), 740 (w), 727 (m), 693 (w). Anal. Calcd (found) for C₃₇H₅₀FeN₅NaO (%): C, 67.36 (66.72); H, 7.63 (7.15); N, 10.62 (10.23). (μ_{eff} = 6.5 μ_B).

Preparation of {2-[2,6-(*i*-Pr)₂PhN=C(CH₃)₂]-6-[2,6-(*i*-Pr)₂PhN=C(CH₃)₂](C₅H₃N)}Fe(μ-N₂)/Na(Et₂O)₃ (2). The LFeCl₂ complex [L = 2,6-[2,6-(*i*-Pr)₂PhN=C(CH₃)₂](C₅H₃N)] was prepared in situ by mixing FeCl₂(THF)_{1.5} (0.100 g, 0.43 mmol) with 2,6-[2,6-(*i*-Pr)₂PhN=C(CH₃)₂](C₅H₃N) (0.205 g, 0.43 mmol) in THF (10 mL) overnight. The dark blue suspension was added to a suspension of NaH (6 equiv, 0.062 g, 2.58 mmol) in THF (5 mL) and stirred for 5 days. The solvent was evaporated, and freshly purified ether added to the dark residue. The mixture was centrifuged to obtain a bright magenta-colored solution, which was separated from the dark precipitates. Dark crystals of **2** grew from the ether extracts upon standing for 2 days at -35 °C (0.225 g, 0.28 mmol, 65% yield). IR (Nujol mull, cm⁻¹): 1965 (s), 1460 (s), 1376 (s), 1292 (m), 1243 (w), 1150 (w), 1097 (m), 1051 (w), 1013 (w), 968 (w), 804 (w), 758 (m), 724 (m), 682 (w). Anal. Calcd (found) for C₄₅H₇₂FeN₅NaO₃ (%): C, 66.73 (66.09); H, 8.95 (8.67); N, 8.65 (8.30). (μ_{eff} = 6.4 μ_B).

Preparation of {2,6-[2,6-(*i*-Pr)₂PhN=C(CH₃)₂](C₅H₃N)}Fe(μ-N₂)/Na[Na(THF)₂] (3). **1. Method A.** The ether-insoluble precipitates from the preparation of **2** were redissolved in THF. The resulting suspension was centrifuged and layered with hexane. After 2 days at room temperature, dark brown crystals of **3** were isolated in 20% yield (0.061 g, 0.08 mmol). IR (Nujol mull, cm⁻¹): 3048

- (16) (a) de Bruin, B.; Bill, E.; Bothe, E.; Weyhermueller, T.; Wieghardt, K. *Inorg. Chem.* **2000**, *39*, 2936. (b) Budzelaar, P. H. M.; de Bruin, B.; Gal A. W.; Wieghardt, K.; van Lenthe, J. H. *Inorg. Chem.* **2001**, *40*, 4649. (c) Knijnenburg, Q.; Hetterscheid, D.; Kooistra, T. M.; Budzelaar, P. H. M. *Eur. J. Inorg. Chem.* **2004**, *6*, 1204.
- (17) Enright, D.; Gambarotta, S.; Yap, G. P. A.; Budzelaar, P. H. M. *Angew. Chem., Int. Ed.* **2002**, *41*, 3873.
- (18) Sugiyama, H.; Korobkov, I.; Gambarotta, S.; Möller, A.; Budzelaar, P. H. M. *Inorg. Chem.* **2004**, *43*, 5771.
- (19) (a) Scott, J.; Gambarotta, S.; Korobkov, I.; Budzelaar, P. H. M. *Organometallics* **2005**, *24*, 6298. (b) Scott, J.; Gambarotta, S.; Korobkov, I.; Knijnenburg, Q.; de Bruin, B.; Budzelaar, P. H. M. *J. Am. Chem. Soc.* **2005**, *127*, 17204. (c) Bouwkamp, M. W.; Bart, S. C.; Hawrelak, E. J.; Trovitch, R. J.; Lobkovsky, E.; Chirik, P. J. *Chem. Commun.* **2005**, 3406.
- (20) Gibson, V. C.; Humphries, M. J.; Tellmann, K. P.; Wass, D. F.; White, A. J. P.; Williams, D. J. *Chem. Commun.* **2001**, 2252.
- (21) Scott, J.; Gambarotta, S.; Korobkov, I. *Can. J. Chem.* **2005**, *83*, 279.
- (22) (a) Archer, A. M.; Bouwkamp, M. W.; Cortez, M.-P.; Lobkovsky, E.; Chirik, P. J. *Organometallics* **2006**, *25*, 4269. (b) Bart, S. C.; Lobkovsky, E.; Bill, E.; Chirik, P. J. *J. Am. Chem. Soc.* **2006**, *128*, 5302. (c) Bart, S. C.; Bowman, A. C.; Lobkovsky, E.; Chirik, P. J. *J. Am. Chem. Soc.* **2007**, *129*, 7212.

- (23) (a) Small, B. L.; Brookhart, M.; Bennett, A. M. A. *J. Am. Chem. Soc.* **1998**, *120*, 4049. (b) Britovsek, G. J. P.; Gibson, V. C.; Kimberley, B. S.; Maddox, P. J.; McTavish, S. J.; Solan, G. A.; White, A. J. P.; Williams, D. J. *Chem. Commun.* **1998**, 849.

(m), 2852 (s), 1899 (s), 1819 (w), 1584 (w), 1540 (w), 1462 (s), 1377 (s), 1356 (m), 1300 (s), 1258 (s), 1201 (w), 1174 (w), 1157 (w), 1095 (m), 1048 (s), 1000 (m), 972 (w), 953 (w), 939 (w), 915 (m), 892 (m), 807 (m), 795 (w), 776 (m), 755 (s), 708 (s), 658 (m). Anal. Calcd (found) for $C_{41}H_{59}FeN_5Na_2O_2$ (%): C, 65.15 (64.79); H, 7.86 (7.85); N, 9.27 (8.90). ($\mu_{\text{eff}} = 5.6 \mu_B$.)

2. Method B. The complex precursor $LFFeCl_2$ was prepared in situ as described above for **2**, and 4 equiv of metallic Na (0.060 g, 2.58 mmol) was added to the THF suspension (15 mL). The mixture was allowed to stir for 1 week, upon which time the color of the solution changed from dark blue to dark orange-brown. The solution was evaporated to dryness, and fresh THF was added to the dark residue. The dark brown solution was centrifuged, concentrated, and layered with hexanes to obtain dark brown crystals of **3** after 2 days at room temperature (0.177 g, 0.23 mmol, 55% yield).

Preparation of {2-[2,6-(*i*Pr)₂PhN=C(CH₃)]-6-[2,6-(*i*Pr)₂PhN-C=CH₂](C₅H₃N)]Fe-N₂ (4). In situ-prepared $LFFeCl_2$ [$FeCl_2$ (THF)_{1.5} (0.250 g, 1.08 mmol) and 2,6-[2,6-(*i*Pr)₂PhN=C(CH₃)]₂(C₅H₃N) (0.514 g, 1.08 mmol) in THF (15 mL)] was reacted with 12 equiv of NaH (0.307 g, 12.8 mmol) in THF (5 mL). The mixture was allowed to stir for 1 week before removing the solvent in vacuo. Hexane (15 mL) was added to the residue and the resulting dark black-brown solution was centrifuged, concentrated to 10 mL, and kept at -35°C . Dark brown-black crystals of **4** were formed after allowing the solution to stand at room temperature for approximately 1 week (0.066 g, 0.12 mmol, 11% yield). IR (Nujol mull, cm^{-1}): 2159 (s), 1576 (s), 1561 (w), 1490 (m), 1460 (s), 1379 (s), 1318 (w), 1269 (s), 1244 (s), 1150 (w), 1109 (m), 1094 (m), 1052 (w), 961 (m), 894 (m), 807 (m), 776 (w), 759 (w), 737 (w), 665 (w). Anal. Calcd (found) for $C_{33}H_{42}FeN_5$ (%): C, 70.08 (69.82); H, 7.66 (7.35); N, 12.39 (12.12). ($\mu_{\text{eff}} = 6.5 \mu_B$.)

Preparation of [{2,6-[2,6-(*i*Pr)₂PhN=C(CH₃)]₂(C₅H₃N)]Fe-N₂]₂(μ -Na)[Na(THF)]₂ (5). The same procedure for the preparation of complex **4** was followed and THF was added to the hexane-insoluble precipitates. The dark brown-orange solution was centrifuged prior to concentrating and layering with hexanes. Dark brown crystals of **5** grew at room temperature within several days (0.091 g, 0.062 mmol, 15% yield per Fe). IR (Nujol mull, cm^{-1}): 2850 (s), 1910 (m), 1868 (m), 1751 (w), 1644 (m), 1586 (w), 1580 (m), 1494 (m), 1466 (s), 1379 (s), 1252 (s), 1179 (m), 1140 (m), 1111 (s), 1094 (s), 1018 (m), 947 (s), 863 (s), 826 (s), 802 (m), 774 (s), 757 (s), 744 (s), 733 (s), 719 (s), 634 (m), 599 (m). Anal. Calcd (found) for $C_{82}H_{118}Fe_2N_{10}Na_3O_4$ (%): C, 66.16 (65.85); H, 7.98 (8.15); N, 9.41 (9.00).

Preparation of {2,6-[2,6-(*i*Pr)₂PhN=C(CH₃)]₂(C₅H₃N)]Fe(μ -1-N₂)(κ^4 -[2,6-[2,6-(*i*Pr)₂PhN=C(CH₃)]₂(NC₅H₂)]Na(THF)₂ (6). Solid samples of $FeCl_2$ (THF)_{1.5} (0.200 g, 0.85 mmol), 2,6-[2,6-(*i*Pr)₂PhN=C(CH₃)]₂(C₅H₃N) (0.820 g, 1.70 mmol), and NaH (0.62 g, 2.55 mmol) were mixed in 30 mL of THF and allowed to stir for 1 week. The color of the solution became dark brown. Evaporation of the solvent afforded a dark brown residue. Addition of fresh hexane and centrifugation lead to the separation of a dark magenta solution. Upon allowing the solution to stand for several days at -35°C , dark magenta crystals of **6** were formed in low yield (0.052 g, 0.043 mmol, 5% yield). IR (Nujol mull, cm^{-1}): 2919 (s), 2853 (s), 2009 (s), 1648 (m), 1614 (s), 1530 (s), 1488 (w), 1461 (s), 1377 (s), 1279 (m), 1237 (m), 1192 (m), 1158 (m), 1120 (s), 1101 (s), 1055 (s), 968 (s), 857 (m), 832 (w), 774 (s), 740 (s), 724 (s), 698 (s), 665 (w), 611 (s). Anal. Calcd (found) for $C_{74}H_{101}FeN_8NaO_2$ (%) solvent-free: C, 73.24 (72.98); H, 8.38 (8.24); N, 9.24 (8.97).

Preparation of {2,6-[2,6-(*i*Pr)₂PhN=C(CH₃)]₂(C₅H₃N)]Fe{2,6-[2,6-(*i*Pr)₂PhN=C(CH₃)]₂(NC₅H₂)]Na(THF)₂ (7). The reaction

was performed as above for the preparation of complex **6**, and the workup was completed as usual to obtain the dark brown solution in hexanes. If the solution is allowed to crystallize at room temperature instead of -35°C , crystals of **7** may be isolated in about 20% yield. Ether can also be added to the left-over insoluble material, and a dark brown solution can be separated by centrifugation. Crystallization at room temperature over the period of a few days afforded more crystals of **7** in about 20% yield, identical in connectivity but displaying a different unit cell than those grown from hexane (0.42 g, 0.33 mmol, combined yield approximately 40%). IR (Nujol mull, cm^{-1}): 1642 (w), 1629 (m), 1617 (m), 1590 (m), 1530 (s), 1461 (s), 1377 (s), 1364 (s), 1327 (m), 1274 (b, m), 1253 (w), 1238 (s), 1190 (m), 1157 (w), 1098 (b, s), 1056 (m), 990 (m), 965 (s), 936 (w), 887 (w), 856 (w), 821 (w), 803 (w), 789 (w), 771 (s), 759 (s), 744 (w), 726 (m), 695 (m), 640 (m). Anal. Calcd (found) for $C_{74}H_{101}FeN_8NaO_2$ (%) solvent-free: C, 81.93 (81.49); H, 9.38 (9.22); N, 7.75 (7.48). ($\mu_{\text{eff}} = 4.5 \mu_B$.)

X-ray Crystallography. All of the compounds consistently yielded crystals that diffracted weakly, and the results presented are the best of several trials. The crystals were mounted on thin glass fibers using paraffin oil and cooled to the data collection temperature. Data were collected on a Bruker AXS SMART 1k CCD diffractometer. Data for the compounds **1**, **2**, **3**, **5**, and **7** were collected with a sequence of 650 scans per set at 0.3° ω scans at 0° , 120° , and 240° in φ . To obtain acceptable redundancy data for compound **6**, the sequence of 650 scans per set with 0.3° ω scans at 0° , 90° , 180° , and 270° in φ was used. Initial unit-cell parameters were determined from 60 data frames collected at the different sections of the Ewald sphere. Semiempirical absorption corrections based on equivalent reflections were applied.²⁴ Systematic absences in the diffraction data set and unit-cell parameters were consistent with monoclinic $P2_1/c$ for **1**, orthorhombic $Pbca$ for **2**, orthorhombic $P2_12_12_1$ for **3**, orthorhombic $P2_12_12_1$ for **4**, monoclinic $P2_1/n$ for **5**, triclinic $P\bar{1}$ for **6**, and orthorhombic $Pbcn$ for **7**. Solutions in centrosymmetric space groups for compounds **1**, **2**, and **6**, and **7**, and noncentrosymmetric for compounds **3** and **4**, yielded chemically reasonable and computationally stable results of refinement. The structures were solved by direct methods, completed with difference Fourier synthesis, and refined with full-matrix least-squares procedures based on F^2 . All non-hydrogen atoms were refined with anisotropic displacement coefficients. All hydrogen atoms were treated as idealized contributions. The unit cell of complex **6** contained 1.5 molecules of disordered hexane which were removed by using SQUEEZE. Complex **7** contains 1.1 molecules of disordered hexane. All scattering factors are contained in several versions of the SHELXTL program library, with the latest version used being v.6.12.²⁵ Crystallographic data and relevant bond distances and angles are reported in Tables 1 and 2.

Calculations. In calculations on mononuclear model systems, the 2,6-*i*Pr₂C₆H₃ groups were replaced by 2,6-Me₂C₆H₃. Spin states up to $S = 5/2$ or $S = 2$ were considered for the naked LFe and (L-H)Fe fragments [L = 2,6-[2,6-Me₂C₆H₃N=C(CH₃)]₂(C₅H₃N); L-H = 2-[2,6-Me₂C₆H₃N=C(CH₃)]-6-[2,6-Me₂C₆H₃N-C=CH₂](C₅H₃N)], and up to $S = 3/2$ or $S = 1$ for the N₂ complexes. Geometries were fully optimized for each individual spin state. All calculations were carried out with the Turbomole program²⁶ coupled to the PQS Baker optimizer.²⁷ All calculations used the spin-unrestricted formalism; even for "S = 0" systems, spin-unrestricted calculations gave significantly lower energies than spin-restricted calculations. Geometries were fully optimized at the B3-LYP level²⁸ using the Turbomole SV(P) basis set^{26a,c} on all atoms. All reported

(24) Blessing, R. *Acta Crystallogr.* **1995**, *A51*, 33.

(25) Sheldrick, G. M. SHELXTL; Bruker AXS: Madison, WI, 2001.

Table 1. Crystal Data and Structure Analysis Results of Complexes 1–7

	1	2	3	4
formula	C ₃₇ H ₅₀ FeN ₅ NaO	C ₄₅ H ₇₂ FeN ₅ NaO ₃	C ₄₁ H ₅₉ FeN ₅ Na ₂ O ₂	C ₃₃ H ₄₂ FeN ₅
mol wt	659.66	809.92	755.76	565.57
cryst syst	monoclinic	orthorhombic	orthorhombic	orthorhombic
space group	<i>P2₁/c</i>	<i>Pbca</i>	<i>P2₁2₁2₁</i>	<i>P2₁2₁2₁</i>
<i>a</i> (Å)	11.816(4)	21.657(8)	12.6462(15)	8.497(4)
<i>b</i> (Å)	16.736(5)	19.805(7)	13.2223(15)	17.870(9)
<i>c</i> (Å)	18.701(6)	22.505(8)	24.765(3)	20.213(11)
α (deg)	90	90	90	90
β (deg)	98.545(6)	90	90	90
γ (deg)	90	90	90	90
<i>V</i> (Å ³)	3657(2)	9653(6)	4141.0(8)	3069(3)
<i>Z</i>	4	8	4	4
radiation (K α , Å)	0.71073	0.71073	0.71073	0.71073
<i>T</i> (K)	213(2)	203(2)	203(2)	203(2)
<i>D</i> _{calcd} (g cm ⁻³)	1.198	1.115	1.212	1.224
μ _{calcd} (mm ⁻¹)	0.459	0.362	0.424	0.521
<i>F</i> ₀₀₀	1408	3504	1616	1208
<i>R</i> , <i>R</i> _w ^{2a}	0.0723, 0.1507	0.0591, 0.1445	0.0492, 0.1044	0.0589, 0.0977
GOF	1.085	1.067	1.051	1.039

	5	6	7
formula	C ₈₂ H ₁₁₈ Fe ₂ N ₁₀ Na ₃ O ₄	C ₇₄ H ₁₀₁ FeN ₈ NaO ₂	C ₇₄ H ₁₀₁ FeN ₆ NaO ₂ ·(hexane) _{1.1}
mol wt	1488.53	1213.47	1287.78
cryst syst	monoclinic	triclinic	orthorhombic
space group	<i>P2₁/n</i>	<i>P1̄</i>	<i>Pbcn</i>
<i>a</i> (Å)	18.343(3)	13.396(4)	20.938(3)
<i>b</i> (Å)	22.444(3)	15.014(5)	25.133(3)
<i>c</i> (Å)	20.117(3)	23.226(7)	30.776(4)
α (deg)	90	71.351(5)	90
β (deg)	95.840(2)	77.270(5)	90
γ (deg)	90	68.453(6)	90
<i>V</i> (Å ³)	8239(2)	4089(2)	16195(3)
<i>Z</i>	4	2	8
radiation (K α , Å)	0.71073	0.71073	0.71073
<i>T</i> (K)	203(2)	206(2)	206(2)
<i>D</i> _{calcd} (g cm ⁻³)	1.200	0.986	1.056
μ _{calcd} (mm ⁻¹)	0.421	0.232	0.237
<i>F</i> ₀₀₀	3188	1308	5595
<i>R</i> , <i>R</i> _w ^{2a}	0.0744, 0.1745	0.0895, 0.2030	0.0759, 0.1677
GOF	1.005	1.002	1.061

$$^a R = \sum |F_o| - |F_c| / \sum |F_o|, R_w = [\sum (|F_o| - |F_c|)^2 / \sum w F_o^2]^{1/2}.$$

energies are electronic energies (frequency calculations were not feasible for these large, open-shell systems).

Description of Structures. Complex 1. Complex **1** consists of a tetracoordinate Fe center (Figure 1) surrounded by the ligand system [Fe(1)–N(1) = 1.904(2) Å, Fe(1)–N(2) = 1.874(2) Å, Fe(1)–N(3) = 1.894(3) Å] and a linearly end-on bound unit of dinitrogen [Fe(1)–N(4) = 1.750(3) Å, Fe(1)–N(4)–N(5) = 177.3(4)°] in a distorted square planar geometry [N(1)–Fe(1)–N(2) =

80.97(11)°, N(1)–Fe(1)–N(3) = 162.29(11)°, N(1)–Fe(1)–N(4) = 98.33(12)°, N(2)–Fe(1)–N(3) = 81.33(11)°, N(2)–Fe(1)–N(4) = 177.33(13)°, N(3)–Fe(1)–N(4) = 99.31(12)°]. In turn, the dinitrogen moiety forms a distorted side-on bridge to a Na atom [N(4)–Na(1) = 2.954(4) Å, N(5)–Na(1) = 2.287(5) Å, Fe(1)–N(4)–Na(1) = 136.17(14)°, N(4)–N(5)–Na(1) = 117.6(3)°, N(5)–N(4)–Na(1) = 43.3(3)°, N(4)–Na(1)–N(5) = 19.09(12)°]. The Na cation is π -bonded to a portion of one aryl ring [Na(1)–C(11) = 2.887(4) Å, Na(1)–C(12) = 2.764(4) Å, Na(1)–C(13) = 2.884(4) Å, Na(1)–C(14) = 3.123(4) Å] and a molecule of THF [Na(1)–O(1) = 2.203(4) Å], as well as being loosely coordinated to the para- and one meta-C of the pyridine ring of a second identical molecule [Na(1)–C(4a) = 2.797(4) Å, Na(1)–C(5a) = 2.772(4) Å] in an overall polymeric array. The N–N bond distance of the bound N₂ unit is 1.090(5) Å, very similar to that of free dinitrogen and indicates minimal or no extent of reduction of the triple bond. The ligand system maintains its planarity but displays modified bond distances throughout the backbone. Most notably, the C_{imine}–C_{methyl} bond lengths have been substantially shortened to 1.446(5) and 1.426(5) Å, indicating deprotonation of one of the methyl groups averaged over the two positions. As expected, the imino functions have also been lengthened as a result of the deprotonation [N(1)–C(2) = 1.376(4) Å, N(3)–C(8) = 1.371(4) Å]. Elongations are apparent in the N_{pyr}–C_{ortho} bonds of the pyridine ring [N(2)–C(3) = 1.365(4) Å, N(2)–C(7) = 1.367(4) Å], along with

- (26) (a) Ahlrichs, R.; Bär, M.; Baron, H.-P.; Bauernschmitt, R.; Böcker, S.; Ehrig, M.; Eichkorn, K.; Elliott, S.; Furche, F.; Haase, F.; Häser, M.; Hättig, C.; Horn, H.; Huber, C.; Huniar, U.; Kattannek, M.; Köhn, A.; Kölmel, C.; Kollwitz, M.; May, K.; Ochsenfeld, C.; Öhm, H.; Schäfer, A.; Schneider, U.; Treutler, O.; Tsereteli, K.; Unterreiner, B.; Von Arnim, M.; Weigend, F.; Weis, P.; Weiss, H. *Turbomole*, version 5; Theoretical Chemistry Group, University of Karlsruhe: Karlsruhe, Germany, 2002. (b) Treutler, O.; Ahlrichs, R. *J. Chem. Phys.* **1995**, *102*, 346–354. (c) Schäfer, A.; Horn, H.; Ahlrichs, R. *J. Chem. Phys.* **1992**, *97*, 2571–2577. (d) Schäfer, A.; Huber, C.; Ahlrichs, R. *J. Chem. Phys.* **1994**, *100*, 5829–5835. (e) Andrae, D.; Haeussermann, U.; Dolg, M.; Stoll, H.; Preuss, H. *Theor. Chim. Acta* **1990**, *77*, 123–141.
- (27) (a) *PQS*, version 2.4; Parallel Quantum Solutions: Fayetteville, AR, 2001 (the Baker optimizer is available separately from PQS upon request). (b) Baker, J. *J. Comput. Chem.* **1986**, *7*, 385–395.
- (28) (a) Lee, C.; Yang, W.; Parr, R. G. *Phys. Rev. B* **1988**, *37*, 785–789. (b) Becke, A. D. *J. Chem. Phys.* **1993**, *98*, 1372–1377. (c) Becke, A. D. *J. Chem. Phys.* **1993**, *98*, 5648–5652. (d) All calculations were performed using the Turbomole functional “b3 lyp”, which is not identical to the Gaussian “B3LYP” functional.

Table 2. Selected Bond Distances (angstroms) and Angles (deg) of Complexes 1–7

1	2	3
Fe(1)–N(1) = 1.904(2)	Fe(1)–N(1) = 1.897(4)	Fe(1)–N(1) = 1.895(4)
Fe(1)–N(2) = 1.874(2)	Fe(1)–N(2) = 1.862(4)	Fe(1)–N(2) = 1.855(4)
Fe(1)–N(3) = 1.894(3)	Fe(1)–N(3) = 1.890(4)	Fe(1)–N(3) = 1.882(4)
Fe(1)–N(4) = 1.750(3)	Fe(1)–N(4) = 1.733(5)	Fe(1)–N(4) = 1.723(5)
N(4)–N(5) = 1.090(5)	N(4)–N(5) = 1.154(6)	N(4)–N(5) = 1.149(6)
N(4)–Na(1) = 2.954(4)	N(5)–Na(1) = 2.389(6)	Na(1)–N(5) = 2.333(5)
N(5)–Na(1) = 2.287(5)	N(1)–C(2) = 1.370(6)	Na(1)–C(24) = 3.050(6)
Na(1)–C(11) = 2.887(4)	N(3)–C(8) = 1.386(6)	Na(1)–C(25) = 2.740(6)
Na(1)–C(12) = 2.764(4)	N(2)–C(3) = 1.376(6)	Na(1)–C(26) = 3.055(6)
Na(1)–C(13) = 2.884(4)	N(2)–C(7) = 1.377(6)	Na(1)–C(2A) = 2.945(6)
Na(1)–C(14) = 3.123(4)	C(1)–C(2) = 1.477(7)	Na(1)–C(3A) = 2.628(5)
Na(1)–O(1) = 2.203(4)	C(2)–C(3) = 1.420(7)	Na(1)–N(2A) = 2.507(5)
Na(1)–C(4a) = 2.797(4)	C(7)–C(8) = 1.427(7)	Na(1)–C(7A) = 3.100(5)
Na(1)–C(5a) = 2.772(4)	C(8)–C(9) = 1.444(7)	Na(1)–Fe(1A) = 3.089(2)
N(1)–C(2) = 1.376(4)	N(1)–Fe(1)–N(2) = 80.97(17)	Na(2)–O(1) = 2.349(5)
N(3)–C(8) = 1.371(4)	N(1)–Fe(1)–N(3) = 161.59(17)	Na(2)–O(2) = 2.328(5)
N(2)–C(3) = 1.365(4)	N(1)–Fe(1)–N(4) = 99.66(18)	Na(2)–N(2) = 2.469(5)
N(2)–C(7) = 1.367(4)	N(2)–Fe(1)–N(3) = 80.63(17)	Na(2)–C(3) = 2.942(6)
C(1)–C(2) = 1.446(5)	N(2)–Fe(1)–N(4) = 174.89(19)	Na(2)–C(7) = 2.732(6)
C(2)–C(3) = 1.436(4)	N(3)–Fe(1)–N(4) = 98.72(18)	Na(2)–Fe(1) = 3.163(3)
C(7)–C(8) = 1.442(4)	Fe(1)–N(4)–N(5) = 177.4(4)	N(1)–C(8) = 1.404(7)
C(8)–C(9) = 1.426(5)	N(4)–N(5)–Na(1) = 171.7(4)	N(3)–C(2) = 1.403(6)
N(1)–Fe(1)–N(2) = 80.97(11)		N(2)–C(3) = 1.433(6)
N(1)–Fe(1)–N(3) = 162.29(11)		N(2)–C(7) = 1.414(6)
N(1)–Fe(1)–N(4) = 98.33(12)		C(1)–C(2) = 1.487(8)
N(2)–Fe(1)–N(3) = 81.33(11)		C(2)–C(3) = 1.389(7)
N(2)–Fe(1)–N(4) = 177.33(13)		C(7)–C(8) = 1.403(7)
N(3)–Fe(1)–N(4) = 99.31(12)		C(8)–C(9) = 1.478(8)
Fe(1)–N(4)–N(5) = 177.3(4)		N(1)–Fe(1)–N(2) = 81.22(18)
Fe(1)–N(4)–Na(1) = 136.17(14)		N(1)–Fe(1)–N(3) = 161.94(19)
N(4)–N(5)–Na(1) = 117.6(3)		N(1)–Fe(1)–N(4) = 101.3(2)
N(5)–N(4)–Na(1) = 43.3(3)		N(2)–Fe(1)–N(3) = 80.79(18)
N(4)–Na(1)–N(5) = 19.09(12)		N(2)–Fe(1)–N(4) = 177.43(19)
		N(3)–Fe(1)–N(4) = 96.67(19)
		Fe(1)–N(4)–N(5) = 174.3(4)
		N(4)–N(5)–Na(1) = 143.4(4)
4	5	5
Fe(1)–N(1) = 1.848(9)	Fe(1)–N(1) = 1.880(6)	C(7)–C(8) = 1.388(11)
Fe(1)–N(2) = 1.775(9)	Fe(1)–N(2) = 1.865(6)	C(8)–C(9) = 1.458(10)
Fe(1)–N(3) = 1.849(9)	Fe(1)–N(3) = 1.883(6)	N(6)–C(35) = 1.386(9)
Fe(1)–N(4) = 1.761(11)	Fe(1)–N(4) = 1.716(7)	N(8)–C(41) = 1.352(9)
N(4)–N(5) = 1.136(12)	Fe(2)–N(6) = 1.881(6)	N(7)–C(36) = 1.388(9)
N(1)–C(2) = 1.379(13)	Fe(2)–N(7) = 1.834(6)	N(7)–C(40) = 1.387(9)
N(3)–C(8) = 1.342(13)	Fe(2)–N(8) = 1.909(6)	C(34)–C(35) = 1.482(11)
N(2)–C(3) = 1.370(13)	Fe(2)–N(9) = 1.782(7)	C(35)–C(36) = 1.389(11)
N(2)–C(7) = 1.386(13)	N(4)–N(5) = 1.163(8)	C(40)–C(41) = 1.411(11)
C(1)–C(2) = 1.468(13)	N(9)–N(10) = 1.112(9)	C(41)–C(42) = 1.513(11)
C(2)–C(3) = 1.425(13)	Na(1)–Fe(1) = 3.034(4)	N(1)–Fe(1)–N(2) = 80.8(3)
C(7)–C(8) = 1.441(14)	Na(1)–O(1) = 2.289(8)	N(1)–Fe(1)–N(3) = 161.4(3)
C(8)–C(9) = 1.441(15)	Na(1)–O(2) = 2.374(8)	N(1)–Fe(1)–N(4) = 97.0(3)
N(1)–Fe(1)–N(2) = 82.1(5)	Na(1)–N(2) = 2.506(7)	N(2)–Fe(1)–N(3) = 80.8(3)
N(1)–Fe(1)–N(3) = 163.2(5)	Na(1)–C(7) = 2.737(8)	N(2)–Fe(1)–N(4) = 177.7(3)
N(1)–Fe(1)–N(4) = 97.7(5)	Na(1)–C(8) = 3.114(9)	N(3)–Fe(1)–N(4) = 101.5(3)
N(2)–Fe(1)–N(3) = 81.2(4)	Na(2)–Fe(1) = 3.045(4)	N(2)–Fe(1)–Na(1) = 55.5(2)
N(2)–Fe(1)–N(4) = 179.8(5)	Na(2)–O(3) = 2.256(10)	N(2)–Fe(1)–Na(2) = 55.4(2)
N(3)–Fe(1)–N(4) = 99.0(5)	Na(2)–O(4) = 2.376(9)	N(4)–Fe(1)–Na(1) = 124.3(2)
	Na(2)–N(2) = 2.511(7)	N(4)–Fe(1)–Na(2) = 125.6(2)
	Na(2)–C(3) = 3.092(9)	Na(1)–Fe(1)–Na(2) = 107.49(11)
	Na(2)–C(7) = 2.626(9)	Fe(1)–N(4)–N(5) = 174.6(7)
	Na(2)–C(8) = 2.954(9)	N(4)–N(5)–Na(3) = 135.4(6)
	Na(3)–Fe(2) = 3.049(4)	N(5)–Na(3)–N(7) = 126.3(3)
	Na(3)–N(5) = 2.336(8)	N(5)–Na(3)–C(13) = 112.7(3)
	Na(3)–C(12) = 3.105(10)	N(6)–Fe(2)–N(7) = 80.7(3)
	Na(3)–C(13) = 2.799(9)	N(6)–Fe(2)–N(8) = 159.1(3)
	Na(3)–C(14) = 3.006(9)	N(6)–Fe(2)–N(9) = 97.7(3)
	Na(3)–N(7) = 2.557(7)	N(7)–Fe(2)–N(8) = 80.4(3)
	Na(3)–C(36) = 3.056(9)	N(7)–Fe(2)–N(9) = 167.5(3)
	Na(3)–C(40) = 2.815(8)	N(8)–Fe(2)–N(9) = 98.8(3)
	N(1)–C(2) = 1.380(9)	Fe(2)–N(9)–N(10) = 178.6(8)
	N(3)–C(8) = 1.402(9)	
	N(2)–C(3) = 1.409(9)	
	N(2)–C(7) = 1.409(9)	
	C(1)–C(2) = 1.492(10)	
	C(2)–C(3) = 1.384(10)	

Table 2. Continued

6	6	7	7
Fe(1)–N(4) = 1.957(4)	C(45)–C(46) = 1.411(7)	Fe(1)–N(1) = 1.916(5)	C(38)–C(39) = 1.427(7)
Fe(1)–N(6) = 1.832(4)	C(46)–C(47) = 1.396(6)	Fe(1)–N(2) = 1.866(4)	C(39)–C(40) = 1.389(7)
Fe(1)–N(14) = 1.947(4)	C(47)–C(48) = 1.383(7)	Fe(1)–N(3) = 1.922(4)	C(40)–C(41) = 1.500(7)
Fe(1)–N(2) = 1.807(6)	C(48)–C(49) = 1.506(7)	Fe(1)–C(38) = 1.939(6)	C(41)–C(42) = 1.514(7)
Fe(1)–C(46) = 1.953(5)	C(49)–C(50) = 1.498(7)	Na(1)–N(4) = 2.508(5)	N(1)–Fe(1)–N(2) = 80.6(2)
Na(39)–N(40) = 2.522(5)	N(4)–Fe(1)–N(6) = 80.3(2)	Na(1)–N(5) = 2.334(5)	N(1)–Fe(1)–N(3) = 159.84(19)
Na(39)–N(44) = 2.350(5)	N(4)–Fe(1)–N(14) = 157.29(18)	Na(1)–N(6) = 2.501(5)	N(1)–Fe(1)–C(38) = 101.0(2)
Na(39)–N(51) = 2.512(5)	N(4)–Fe(1)–N(2) = 98.2(2)	Na(1)–O(1) = 2.283(5)	N(2)–Fe(1)–N(3) = 80.4(2)
Na(39)–O(76) = 2.350(5)	N(4)–Fe(1)–C(46) = 98.88(19)	Na(1)–O(2) = 2.318(6)	N(2)–Fe(1)–C(38) = 169.0(2)
Na(39)–O(81) = 2.288(5)	N(6)–Fe(1)–N(14) = 80.02(19)	N(1)–C(8) = 1.379(7)	N(3)–Fe(1)–C(38) = 99.0(2)
N(2)–N(3) = 1.133(6)	N(6)–Fe(1)–N(2) = 162.55(18)	N(3)–C(2) = 1.367(7)	N(4)–Na(1)–N(5) = 66.58(16)
N(4)–C(5) = 1.355(7)	N(6)–Fe(1)–C(46) = 102.1(2)	N(2)–C(3) = 1.373(7)	N(4)–Na(1)–N(6) = 129.87(17)
N(14)–C(12) = 1.360(6)	N(14)–Fe(1)–N(2) = 97.26(19)	N(2)–C(7) = 1.362(7)	N(4)–Na(1)–O(1) = 114.25(19)
N(6)–C(7) = 1.373(7)	N(14)–Fe(1)–C(46) = 96.16(18)	C(1)–C(2) = 1.498(8)	N(4)–Na(1)–O(2) = 102.3(2)
N(6)–C(11) = 1.398(6)	N(2)–Fe(1)–C(46) = 95.3(2)	C(2)–C(3) = 1.420(8)	N(5)–Na(1)–N(6) = 66.56(16)
C(6)–C(5) = 1.525(8)	Fe(1)–N(2)–N(3) = 178.7(5)	C(7)–C(8) = 1.398(8)	N(5)–Na(1)–O(1) = 157.9(2)
C(5)–C(7) = 1.408(8)	N(40)–Na(39)–N(44) = 67.02(15)	C(8)–C(9) = 1.522(8)	N(5)–Na(1)–O(2) = 98.4(2)
C(11)–C(12) = 1.387(7)	N(40)–Na(39)–N(51) = 132.85(16)	N(4)–C(35) = 1.282(6)	N(6)–Na(1)–O(1) = 102.76(18)
C(12)–C(13) = 1.492(7)	N(40)–Na(39)–O(76) = 97.10(17)	N(6)–C(41) = 1.275(6)	N(6)–Na(1)–O(2) = 101.10(19)
N(40)–C(41) = 1.282(7)	N(40)–Na(39)–O(81) = 106.69(17)	N(5)–C(36) = 1.353(6)	O(1)–Na(1)–O(2) = 102.8(2)
N(51)–C(49) = 1.290(6)	N(44)–Na(39)–N(51) = 67.28(15)	N(5)–C(40) = 1.332(6)	
N(44)–C(43) = 1.369(6)	N(44)–Na(39)–O(76) = 101.21(18)	C(34)–C(35) = 1.511(7)	
N(44)–C(48) = 1.347(6)	N(44)–Na(39)–O(81) = 159.0(2)	C(35)–C(36) = 1.489(7)	
C(42)–C(41) = 1.508(7)	N(51)–Na(39)–O(76) = 102.44(17)	C(36)–C(37) = 1.381(7)	
C(41)–C(43) = 1.501(7)	N(51)–Na(39)–O(81) = 111.73(18)	C(37)–C(38) = 1.397(7)	
C(43)–C(45) = 1.373(7)	O(76)–Na(39)–O(81) = 99.4(2)		

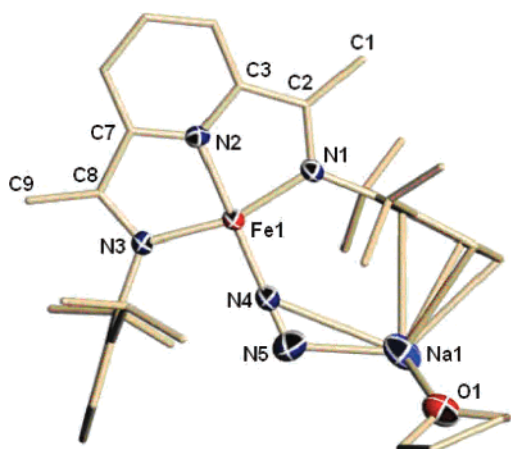


Figure 1. Partial thermal ellipsoid plot of complex **1**, drawn at the 50% probability level. Hydrogen atoms have been omitted for clarity.

contractions in the $C_{\text{imine}}-C_{\text{ortho}}$ bond lengths [C(2)–C(3) = 1.436(4) Å, C(7)–C(8) = 1.442(4) Å]. These distances diagnose substantial reduction of the ligand.^{14,16}

Complex 2. The structure of complex **2** is closely related to that of **1**. The Fe center is coordinated to the ligand system [Fe(1)–N(1) = 1.897(4) Å, Fe(1)–N(2) = 1.862(4) Å, Fe(1)–N(3) = 1.890(4) Å] and to an end-on dinitrogen unit [Fe(1)–N(4) = 1.733(5) Å] in a distorted square planar geometry [N(1)–Fe(1)–N(2) = 80.97(17)°, N(1)–Fe(1)–N(3) = 161.59(17)°, N(1)–Fe(1)–N(4) = 99.66(18)°, N(2)–Fe(1)–N(3) = 80.63(17)°, N(2)–Fe(1)–N(4) = 174.89(19)°, N(3)–Fe(1)–N(4) = 98.72(18)°]. Structural differences to complex **1** involve the environment of the Na counterion. In this case, the Na ion is coordinated to the second nitrogen atom of the bridging dinitrogen [N(5)–Na(1) = 2.389(6) Å, Fe(1)–N(4)–N(5) = 177.4(4)°, N(4)–N(5)–Na(1) = 171.7(4)°] and solvated by three molecules of ether. The dinitrogen unit displays a slight elongation compared to free dinitrogen [N(4)–N(5) = 1.154(6) Å] and is coordinated to the Fe center through a fairly short bond [Fe(1)–N(4) = 1.733(5) Å]. One of the two imino-methyl groups of the ligand backbone appears to have been deprotonated [C(1)–C(2) = 1.477(7) Å and C(8)–C(9) = 1.444-

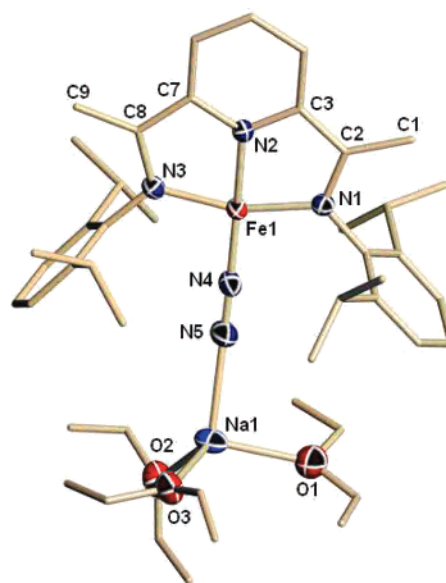


Figure 2. Partial thermal ellipsoid plot of complex **2**, drawn at the 50% probability level. Hydrogen atoms have been omitted for clarity.

(7) Å]. Also, other bond distances and angles of the ligand suggest some degree of reduction throughout the backbone, being characterized by a contraction in the $C_{\text{imine}}-C_{\text{ortho}}$ bond lengths [C(2)–C(3) = 1.420(7) Å and C(7)–C(8) = 1.427(7) Å] and elongation in the imine bonds [N(1)–C(2) = 1.370(6) Å and N(3)–C(8) = 1.386(6) Å] as well as the $N_{\text{pyr}}-C_{\text{ortho}}$ bonds [N(2)–C(3) = 1.376(6) Å and N(2)–C(7) = 1.377(6) Å].

Complex 3. The ligand system in complex **3** chelates the Fe center (Figure 3) in a distorted square planar arrangement [Fe(1)–N(1) = 1.895(4) Å, Fe(1)–N(2) = 1.855(4) Å, Fe(1)–N(3) = 1.882(4) Å]. The fourth coordination site is occupied by an end-on dinitrogen unit [Fe(1)–N(4) = 1.723(5) Å, N(1)–Fe(1)–N(2) = 81.22(18)°, N(1)–Fe(1)–N(3) = 161.94(19)°, N(1)–Fe(1)–N(4) = 101.3(2)°, N(2)–Fe(1)–N(3) = 80.79(18)°, N(2)–Fe(1)–N(4) = 177.43(19)°, N(3)–Fe(1)–N(4) = 96.67(19)°]. The N–N distance [N(4)–N(5) = 1.149(6) Å] is still very short and suggests

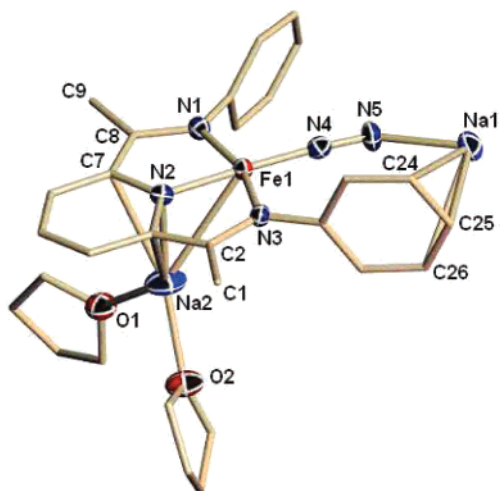


Figure 3. Partial thermal ellipsoid plot of complex **3**, drawn at the 50% probability level. ⁱPr substituents on the aryl rings and all hydrogen atoms have been omitted for clarity.

only a minor degree of activation of the triple bond. The bonding of the dinitrogen unit to the metal center is slightly bent [$\text{Fe}(1)\text{--N}(4)\text{--N}(5) = 174.3(4)^\circ$] and forms a bridge to a Na atom [$\text{Na}(1)\text{--N}(5) = 2.333(5) \text{ \AA}$, $\text{N}(4)\text{--N}(5)\text{--Na}(1) = 143.4(4)^\circ$]. Unlike complex **1**, in this case the dinitrogen unit forms a slightly bent end-on bridge to the Na, as opposed to the distorted side-on binding seen in **1**. The Na atom is coordinated (η^3 -) to the meta- and para-carbons of one of the aryl groups of the ligand [$\text{Na}(1)\text{--C}(24) = 3.050(6) \text{ \AA}$, $\text{Na}(1)\text{--C}(25) = 2.740(6) \text{ \AA}$, $\text{Na}(1)\text{--C}(26) = 3.055(6) \text{ \AA}$], as well as η^3 - to the N_{pyr} , C_{ortho} , and C_{imine} of a second molecule [$\text{Na}(1)\text{--N}(2\text{A}) = 2.507(5) \text{ \AA}$, $\text{Na}(1)\text{--C}(3\text{A}) = 2.628(5) \text{ \AA}$, $\text{Na}(1)\text{--C}(2\text{A}) = 2.945(6) \text{ \AA}$, $\text{Na}(1)\text{--C}(7\text{A}) = 3.100(5) \text{ \AA}$], thereby assembling a polymeric array. A second Na atom is present, η^3 -bound to the pyridine N and ortho-C's of the ligand [$\text{Na}(2)\text{--N}(2) = 2.469(5) \text{ \AA}$, $\text{Na}(2)\text{--C}(3) = 2.942(6) \text{ \AA}$, $\text{Na}(2)\text{--C}(7) = 2.732(6) \text{ \AA}$] and solvated by two molecules of THF [$\text{Na}(2)\text{--O}(1) = 2.349(5) \text{ \AA}$, $\text{Na}(2)\text{--O}(2) = 2.328(5) \text{ \AA}$]. The coordination of two Na atoms to the delocalized π -system of the ligand is paralleled by modifications to the ligand bond distances. The imine bond distances have been lengthened substantially in comparison to the neutral ligand [$\text{N}(1)\text{--C}(8) = 1.404(7) \text{ \AA}$, $\text{N}(3)\text{--C}(2) = 1.403(6) \text{ \AA}$], as have the $\text{N}_{\text{pyr}}\text{--C}_{\text{ortho}}$ bond lengths [$\text{N}(2)\text{--C}(3) = 1.433(6) \text{ \AA}$, $\text{N}(2)\text{--C}(7) = 1.414(6) \text{ \AA}$]. These elongations are also paralleled by a contraction in the $\text{C}_{\text{imine}}\text{--C}_{\text{ortho}}$ bonds [$\text{C}(2)\text{--C}(3) = 1.389(7) \text{ \AA}$, $\text{C}(7)\text{--C}(8) = 1.403(7) \text{ \AA}$]. The $\text{C}_{\text{imine}}\text{--C}_{\text{methyl}}$ bond lengths are similar to those of the neutral ligand [$\text{C}(1)\text{--C}(2) = 1.487(8) \text{ \AA}$, $\text{C}(8)\text{--C}(9) = 1.478(8) \text{ \AA}$] and exclude deprotonation.

Complex 4. The structure of complex **4** (Figure 4) consists of the tridentate ligand system surrounding the Fe center in a distorted square planar coordination geometry [$\text{Fe}(1)\text{--N}(1) = 1.848(9) \text{ \AA}$, $\text{Fe}(1)\text{--N}(2) = 1.775(9) \text{ \AA}$, $\text{Fe}(1)\text{--N}(3) = 1.849(9) \text{ \AA}$]. A terminally bound end-on dinitrogen unit [$\text{Fe}(1)\text{--N}(4) = 1.761(11) \text{ \AA}$, $\text{N}(1)\text{--Fe}(1)\text{--N}(2) = 82.1(5)^\circ$, $\text{N}(1)\text{--Fe}(1)\text{--N}(3) = 163.2(5)^\circ$, $\text{N}(1)\text{--Fe}(1)\text{--N}(4) = 97.7(5)^\circ$, $\text{N}(2)\text{--Fe}(1)\text{--N}(3) = 81.2(4)^\circ$, $\text{N}(2)\text{--Fe}(1)\text{--N}(4) = 179.8(5)^\circ$, $\text{N}(3)\text{--Fe}(1)\text{--N}(4) = 99.0(5)^\circ$] completes the structure. The N–N distance shows a minor elongation compared to free dinitrogen [$\text{N}(4)\text{--N}(5) = 1.136(12) \text{ \AA}$], while the relatively short Fe– N_2 distance suggests substantial degree of back-bonding. The $\text{C}_{\text{imine}}\text{--C}_{\text{methyl}}$ bond lengths [$\text{C}(1)\text{--C}(2) = 1.468(13) \text{ \AA}$, $\text{C}(8)\text{--C}(9) = 1.441(15) \text{ \AA}$] indicate a scenario similar to **1** and **2**. Other bond distances of the ligand backbone are indicative of reduction of the ligand [$\text{N}(1)\text{--C}(2) = 1.379(13) \text{ \AA}$, $\text{N}(3)\text{--C}(8)$

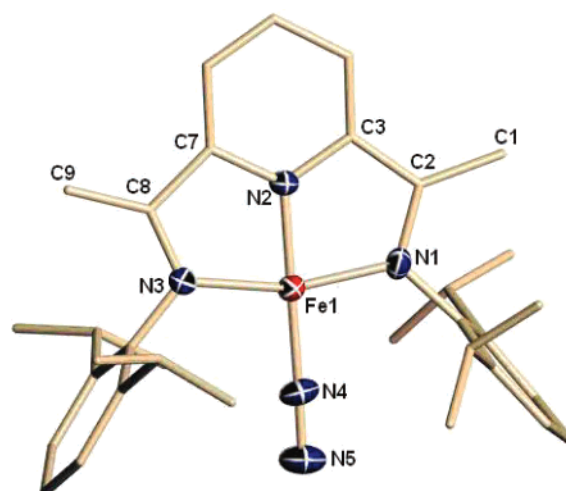


Figure 4. Thermal ellipsoid plot of complex **4**, drawn at the 50% probability level.

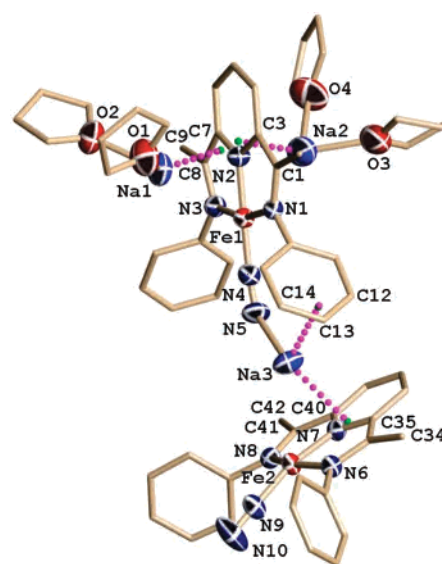


Figure 5. Partial thermal ellipsoid plot of complex **5**, drawn at the 50% probability level. ⁱPr substituents on the aryl rings and all hydrogen atoms have been omitted for clarity.

$= 1.342(13) \text{ \AA}$, $\text{C}(2)\text{--C}(3) = 1.425(13) \text{ \AA}$, $\text{C}(7)\text{--C}(8) = 1.441(14) \text{ \AA}$, $\text{N}(2)\text{--C}(3) = 1.370(13) \text{ \AA}$, $\text{N}(2)\text{--C}(7) = 1.386(13) \text{ \AA}$].

Complex 5. The structure of complex **5** features two ligand systems, two Fe centers, three Na atoms, and two end-on bound dinitrogen moieties (Figure 5). The first Fe center adopts a distorted square planar geometry comprising the three N atoms of the first ligand system [$\text{Fe}(1)\text{--N}(1) = 1.880(6) \text{ \AA}$, $\text{Fe}(1)\text{--N}(2) = 1.865(6) \text{ \AA}$, $\text{Fe}(1)\text{--N}(3) = 1.883(6) \text{ \AA}$] and an end-on dinitrogen unit [$\text{Fe}(1)\text{--N}(4) = 1.716(7) \text{ \AA}$, $\text{N}(1)\text{--Fe}(1)\text{--N}(2) = 80.8(3)^\circ$, $\text{N}(1)\text{--Fe}(1)\text{--N}(3) = 161.4(3)^\circ$, $\text{N}(1)\text{--Fe}(1)\text{--N}(4) = 97.0(3)^\circ$, $\text{N}(2)\text{--Fe}(1)\text{--N}(3) = 80.8(3)^\circ$, $\text{N}(2)\text{--Fe}(1)\text{--N}(4) = 177.7(3)^\circ$, $\text{N}(3)\text{--Fe}(1)\text{--N}(4) = 101.5(3)^\circ$]. The dinitrogen unit forms a slightly bent array with the Fe center [$\text{Fe}(1)\text{--N}(4)\text{--N}(5) = 174.6(7)^\circ$] and displays a N–N bond length [$\text{N}(4)\text{--N}(5) = 1.163(8) \text{ \AA}$] indicative of minimum extent of activation. Two Na atoms, each solvated by two molecules of THF [$\text{Na}(1)\text{--O}(1) = 2.289(8) \text{ \AA}$, $\text{Na}(1)\text{--O}(2) = 2.374(8) \text{ \AA}$, $\text{Na}(2)\text{--O}(3) = 2.256(10) \text{ \AA}$, $\text{Na}(2)\text{--O}(4) = 2.376(9) \text{ \AA}$], coordinate to the first ligand system, each being perpendicularly placed to one of the two sides of the plane defined by the pyridine ring and the ligand backbone. The first Na atom appears to be η^3 -bound to the N_{pyr} , C_{ortho} , and adjacent C_{imine} [$\text{Na}(1)\text{--N}(2)$

= 2.506(7) Å, Na(1)–C(7) = 2.737(8) Å, Na(1)–C(8) = 3.114(9) Å] while the second Na atom coordinates to the same atoms from the opposite side, forming an additional short contact with the other ortho-C atom [Na(2)–N(2) = 2.511(7) Å, Na(2)–C(3) = 3.092(9) Å, Na(2)–C(7) = 2.626(9) Å, Na(2)–C(8) = 2.954(9) Å]. A third Na atom is connected to the first molecule via an end-on dinitrogen bridge to the Fe center [Na(3)–N(5) = 2.336(8) Å, N(4)–N(5)–Na(3) = 135.4(6)°] and a π -coordination to the aryl group of the first ligand [Na(3)–C(12) = 3.105(10) Å, Na(3)–C(13) = 2.799(9) Å, Na(3)–C(14) = 3.006(9) Å]. In turn, the same atom is also coordinated to a portion of the pyridine ring of a second unit [Na(3)–N(7) = 2.557(7) Å, Na(3)–C(36) = 3.056(9) Å, Na(3)–C(40) = 2.815(8) Å] formed by the second ligand bonded to the other Fe–N₂ unit [Fe(2)–N(6) = 1.881(6) Å, Fe(2)–N(7) = 1.834(6) Å, Fe(2)–N(8) = 1.909(6) Å, Fe(2)–N(9) = 1.782(7) Å, N(6)–Fe(2)–N(7) = 80.7(3)°, N(6)–Fe(2)–N(8) = 159.1(3)°, N(6)–Fe(2)–N(9) = 97.7(3)°, N(7)–Fe(2)–N(8) = 80.4(3)°, N(7)–Fe(2)–N(9) = 167.5(3)°, N(8)–Fe(2)–N(9) = 98.8(3)°]. The coordination of the N₂ ligand in this second unit is almost linear [Fe(2)–N(9)–N(10) = 178.6(8)°] with only a small degree of N–N triple bond activation [N(9)–N(10) = 1.112(9) Å]. The two ligand systems display slight differences in the bond lengths of the backbone. Both exhibit elongated N_{imine}–C_{imine} [N(1)–C(2) = 1.380(9) Å, N(3)–C(8) = 1.402(9) Å, N(6)–C(35) = 1.386(9) Å, N(8)–C(41) = 1.352(9) Å] and N_{pyr}–C_{ortho} bond distances [N(2)–C(3) = 1.409(9) Å, N(2)–C(7) = 1.409(9) Å, N(7)–C(36) = 1.388(9) Å, N(7)–C(40) = 1.387(9) Å]. The C_{imine}–C_{ortho} bonds fall in the range expected for reduced complexes [C(2)–C(3) = 1.384(10) Å, C(7)–C(8) = 1.388(11) Å, C(35)–C(36) = 1.389(11) Å, C(40)–C(41) = 1.411(11) Å]. Deviations from the normal geometry occur to a larger extent at the first ligand system, as expected for an increased electron density in the ligand π^* orbitals.^{14,16} In this case the C_{Me}–C_{imine} distances exclude deprotonation [C(1)–C(2) = 1.492(10) Å, C(8)–C(9) = 1.458(10) Å, C(34)–C(35) = 1.482(11) Å, C(41)–C(42) = 1.513(11) Å].

Complex 6. Complex 6 consists of two distinct moieties. The first is composed of one ligand surrounding one Fe–N₂ unit. The second is formed by another ligand chelating one Na atom solvated by two molecules of THF. The link between the two units is made by a σ -bond between the Fe of the first unit and the pyridine C_{para} atom of the second. Given the perfect coplanarity of this pyridine ring with the metal center, it is obvious that the corresponding H atom has been removed (Figure 6). The Fe center adopts a square pyramidal geometry ($\tau = 0.09$)²⁹ defined by the three nitrogen atoms of the ligand backbone [Fe(1)–N(4) = 1.957(4) Å, Fe(1)–N(6) = 1.832(4) Å, Fe(1)–N(14) = 1.947(4) Å] and one N atom of a terminal end-on dinitrogen unit [Fe(1)–N(2) = 1.807(6) Å, N(4)–Fe(1)–N(6) = 80.3(2)°, N(4)–Fe(1)–N(14) = 157.29(18)°, N(4)–Fe(1)–N(2) = 98.2(2)°, N(6)–Fe(1)–N(14) = 80.02(19)°, N(6)–Fe(1)–N(2) = 162.55(18)°, N(14)–Fe(1)–N(2) = 97.26(19)°]. The apical position is occupied by the C_{para} of the pyridine ring of the second unit [Fe(1)–C(46) = 1.953(5) Å]. The planar backbone of the second ligand is oriented orthogonally to the first ligand plane [Na(39)–N(40) = 2.522(5) Å, Na(39)–N(44) = 2.350(5) Å, Na(39)–N(51) = 2.512(5) Å, Na(39)–O(76) = 2.350(5) Å, Na(39)–O(81) = 2.288(5) Å]. The geometry about the Na atom can be regarded as distorted either square pyramidal or trigonal bipyramidal ($\tau = 0.44$)²⁹ [N(40)–Na(39)–N(44) = 67.02(15)°, N(40)–Na(39)–N(51) = 132.85(16)°, N(40)–Na(39)–O(76) = 97.10(17)°, N(40)–Na(39)–O(81) = 106.69(17)°, N(44)–Na(39)–N(51) = 67.28(15)°, N(44)–Na(39)–O(76) = 101.21(18)°, N(44)–Na(39)–O(81)

(29) Addison, A. W.; Rao, T. N.; Reedijk, J.; van Rijn, J.; Verschoor, G. C. *J. Chem. Soc., Dalton Trans.* **1984**, 1349.

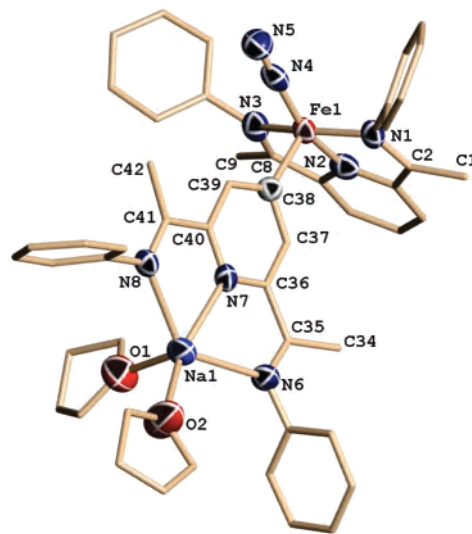


Figure 6. Partial thermal ellipsoid plot of complex 6, drawn at the 50% probability level. ⁱPr substituents on the aryl rings and all hydrogen atoms have been omitted for clarity.

= 159.0(2)°, N(51)–Na(39)–O(76) = 102.44(17)°, N(51)–Na(39)–O(81) = 111.73(18)°, O(76)–Na(39)–O(81) = 99.4(2)°]. In the case of the second ligand system, the bond lengths of the backbone are barely changed with respect to the free ligand and do not require further discussion. However, the bond distances of the ligand surrounding the Fe center show significant perturbations in comparison to the neutral ligand. The imine C=N and N_{pyr}–C_{ortho} bond lengths [N(4)–C(5) = 1.355(7) Å, N(14)–C(12) = 1.360(6) Å, N(6)–C(7) = 1.373(7) Å, N(6)–C(11) = 1.398(6) Å] appear to be elongated, whereas the C_{imine}–C_{ortho} bond lengths [C(5)–C(7) = 1.408(8) Å, C(11)–C(12) = 1.387(7) Å] are shortened, suggesting a substantial amount of electron transfer to the ligand system.^{14,16} The C_{imine}–C_{methyl} bonds are in the normal range of C–C single bonds [C(5)–C(6) = 1.525(8) Å, C(12)–C(13) = 1.492(7) Å, C(41)–C(42) = 1.508(7) Å, C(49)–C(50) = 1.498(7) Å]. The end-on bound dinitrogen unit shows a fairly short N–N bond distance [N(2)–N(3) = 1.133(6) Å] in line with the other complexes.

Complex 7. The structure of complex 7 is very similar, from the chemical point of view, to that of complex 6, the only difference being the absence of the N₂ (Figure 7). The Fe center forms bonds to the three nitrogen atoms of the first ligand system [Fe(1)–N(1) = 1.916(5) Å, Fe(1)–N(2) = 1.866(4) Å, Fe(1)–N(3) = 1.922(4) Å]. The fourth coordination site of its distorted square planar geometry [N(1)–Fe(1)–N(2) = 80.6(2)°, N(1)–Fe(1)–N(3) = 159.84(19)°, N(1)–Fe(1)–C(38) = 101.0(2)°, N(2)–Fe(1)–N(3) = 80.4(2)°, N(2)–Fe(1)–C(38) = 169.0(2)°, N(3)–Fe(1)–C(38) = 99.0(2)°] is defined by the pyridine para-C of the second ligand [Fe(1)–C(38) = 1.939(6) Å] perfectly coplanar with the metal center. The Na atom coordinates to the three nitrogen atoms of the second ligand [Na(1)–N(4) = 2.508(5) Å, Na(1)–N(5) = 2.334(5) Å, Na(1)–N(6) = 2.501(5) Å] and two molecules of THF [Na(1)–O(1) = 2.283(5) Å, Na(1)–O(2) = 2.318(6) Å] in a penta-coordinate arrangement ($\tau = 0.47$)²⁹ [N(4)–Na(1)–N(5) = 66.58(16)°, N(4)–Na(1)–N(6) = 129.87(17)°, N(4)–Na(1)–O(1) = 114.25(19)°, N(4)–Na(1)–O(2) = 102.3(2)°, N(5)–Na(1)–N(6) = 66.56(16)°, N(5)–Na(1)–O(1) = 157.9(2)°, N(5)–Na(1)–O(2) = 98.4(2)°, N(6)–Na(1)–O(1) = 102.76(18)°, N(6)–Na(1)–O(2) = 101.10(19)°, O(1)–Na(1)–O(2) = 102.8(2)°]. The trigonal planar geometry of the para-C_{pyridine} on the second ligand implies that even in this case the corresponding H atom has been removed. No other

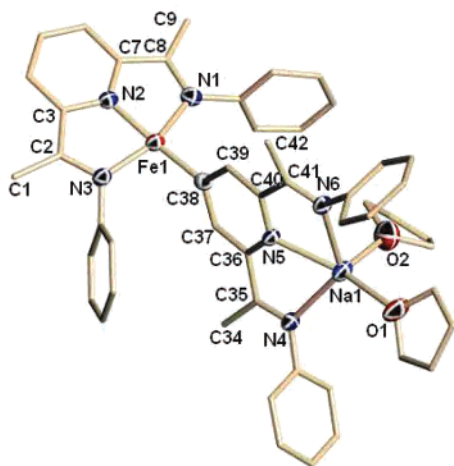
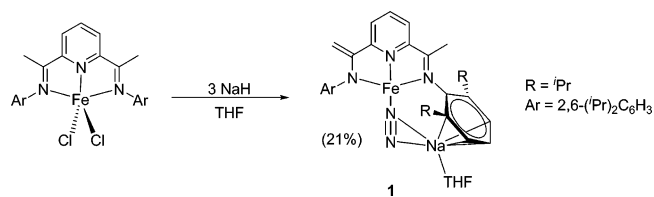


Figure 7. Partial thermal ellipsoid plot of complex **7**, drawn at the 50% probability level. ^tPr substituents on the aryl rings and all hydrogen atoms have been omitted for clarity.

Scheme 2



ligand modifications are apparent in the bond distances and angles of the backbone. As in **6**, the ligand system surrounding the Fe atom displays backbone modifications as expected for substantial charge transfer from the metal to the ligand.^{14,16}

Results and Discussion

The reduction of LFeCl_2 { $\text{L} = 2,6\text{-}[2,6\text{-}(\text{tPr})_2\text{PhN}=\text{C}(\text{CH}_3)]_2(\text{C}_5\text{H}_3\text{N})$ } with 3 equiv of NaH in THF afforded a bright burgundy reaction mixture containing a distribution of products. An ether-soluble portion of the reaction mixture gave the paramagnetic $\{2\text{-}[2,6\text{-}(\text{tPr})_2\text{PhN}=\text{C}(\text{CH}_3)]\text{-}6\text{-}[2,6\text{-}(\text{tPr})_2\text{PhN}-\text{C}=\text{CH}_2](\text{C}_5\text{H}_3\text{N})\}\text{Fe}(\mu\text{-}\eta^2\text{-N}_2)\text{Na}(\text{THF})$ (**1**) in moderate yield (Scheme 2). Crystals suitable for X-ray diffraction were shown to be very prone toward spontaneous loss of gas, as witnessed by a continuous foaming on the surface of the crystals, even at low temperature. In spite of all precautions, rapid deterioration of the crystals prevented collection of a satisfactory data set. Only in one instance were crystals of sufficient quality obtained for determination of the connectivity (Figure 1).

The imine-methyl C–C distances indicate that the ligand is monodeprotonated, and consequently monoanionic, with the $\text{C}=\text{CH}_2$ group disordered over the two positions. The possibility that the terminal N atom may bear one or more H atoms, as suggested by the bending of the $\text{Fe}-\text{N}_2-\text{Na}$ vector, was clearly ruled out by the IR spectrum, which does not show an N–H stretch. Therefore, from the formal point of view, complex **1** can be described as the combination of a zero-valent Fe center surrounded by a monodeprotonated monoanionic ligand and an end-on bound dinitrogen moiety with a π -bonded sodium counterion. In fact, the distorted square planar coordination geometry about Fe is very similar

to that of the two-electron-reduced complex $[\text{LFeMe}][\text{Li}(\text{THF})_4]$ ^{19a} and might be consistent with the presence of a formal d^8 zero-valent Fe. On the other hand, given the established ability of this particular ligand system to accept electron density into the delocalized π -system and to form radical anions,^{14,16–19} the complex can be more realistically described as containing the metal center in a higher oxidation state partially coupled to a reduced form of the ligand. The room-temperature magnetic moment ($\mu_{\text{eff}} = 6.5 \mu_{\text{B}}$) is intriguingly high. Such value would imply an electronic configuration for the metal of about five unpaired electrons, which is quite hard to reconcile with any oxidation state lower than Fe(III). The real oxidation state of Fe can be at most divalent (four unpaired electrons). With the deprotonated ligand as -1 and Na as $+1$, there must then be two additional electrons on the ligand. They would be in different orbitals and couple antiferromagnetically to the metal which leaves the complex with a net $S = 1$ at most, as correctly proposed by Bart et al. for the double-dinitrogen complex of the same ligand.⁸ Computational results (see below) consistently attributed the lower energy to the lowest spin states. Thus, the high room-temperature magnetism can be attributed to thermal population from the low-lying low-spin state. Incidentally, this behavior is also consistent with that of the previously reported $[\text{LFeMe}][\text{Li}(\text{THF})_4]$,^{19a} also with a formal appearance of a zero-valent species and whose magnetic moment spectacularly rises from 1.30 to 6.45 μ_{BM} as a function of the temperature increase to ambient values. However, as is often the case for these reduced complexes, the presence of undetectable amount of metallic impurities, largely affecting the measurements, cannot be excluded.

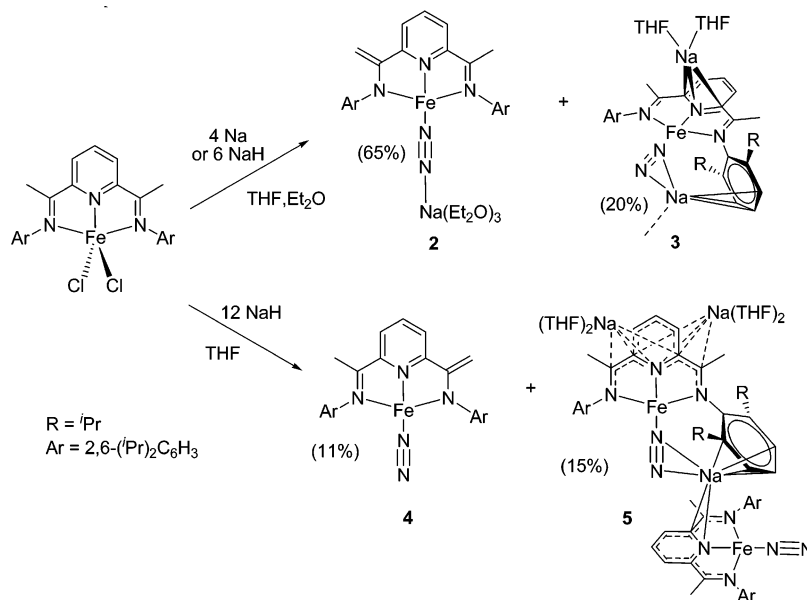
The features of the coordinated nitrogen are also rather intriguing, if not somewhat contradictory (Table 3). The N–N distance [1.090(5) Å] indicates minimal, if any, reduction of the N–N triple bond. In sharp contrast, however, the N–N stretching frequency of 1912 cm^{-1} is substantially lower than in other terminally bonded Fe–dinitrogen complexes^{5a–g,i,j} and might indicate at least some reduction of the N–N bond order. Furthermore, the remarkably short Fe–N₂ bond distance [1.750(3) Å] also suggests possible Fe–N multiple bond character. These features are slightly in contrast with those of the Bart et al.'s double-dinitrogen complex of the very same ligand system.⁸ Although the N–N distances are very comparable, the N₂ stretching frequencies appear to be at substantially lower frequencies. Among the series of dinitrogen complexes reported in this work, only complex **4** (vide infra), which does not contain coordinated Na, displays comparable N₂ stretching frequency to the double-dinitrogen complex and yet a somewhat longer N–N distance. Thus, the N–N distance is a poor criterion for these complexes to assess the extent of activation.

As indicated by the recent results in dinitrogen reduction/cleavage obtained upon similar reduction with the Cr analogue,¹⁵ the amount of NaH used is critical for the formation and isolation of species carrying a different extent of reduction and otherwise formed under identical reaction conditions. Thus, reduction of the dichloride precursor with 6 equiv of NaH in THF afforded two other dinitrogen

Table 3. Comparative Bond Distances and N–N Stretching Frequencies of LFeN₂ Complexes and Other Crystallographically Characterized Fe–N₂ Complexes^a

compd	Fe–N (Å)	N–N (Å)	ν (N–N) (cm ⁻¹)
1	1.750(3)	1.090(5)	1912
2	1.733(5)	1.154(6)	1965
3	1.723(5)	1.149(6)	1899
4	1.761(11)	1.136(12)	2159
5 Fe(1)–N ₂	1.716(7)	1.163(8)	1868
5 Fe(2)–N ₂	1.782(7)	1.112(9)	1910
6	1.807(6)	1.133(6)	2009
LFe(N ₂) ₂ (first) ^b	1.8341(16)	1.090(2)	2124
LFe(N ₂) ₂ (second) ^b	1.8800(19)	1.104(3)	2053
<chgrow;lp;4q> <i>trans</i> -[FeH(N ₂)(dmpc)] [BPh ₄] ^c	1.818(11) ^d	1.13(3)a	2094
Fe(N ₂)(depe) ₂ ^e	1.748(8)	1.139(13)	1955
[Fe(η^5 -C ₅ H ₅)(N ₂)(dippe)] [BPh ₄] ^f	1.76(1)	1.13(1)	2112
[FeH(N ₂)(NP ₃)] [BPh ₄] ^g	1.809(9)	1.102(13)	2090
[FeCl(N ₂)(depe) ₂] [BPh ₄] ^h	1.784(9)	1.073(11)	2088
Fe(CNC)(N ₂) ₂ (first) ⁱ	1.847(2)	1.115(3)	2031
Fe(CNC)(N ₂) ₂ (second) ⁱ	1.820(2)	1.113(3)	2109
Fe(H) ₂ (N ₂)(PEtPh ₂) ₃ ^j	1.786(7)	1.136(7)	2043
[FeH(N ₂)(P ₄)] [Br] ^k	1.865(15)	1.076(15)	2130
{[PhBP ^{Pr} ₃]Fe} ₂ (μ -N ₂) ^l	1.814(5) ^d	1.138(5)	
{([PhBP ^{Pr} ₃]Fe) ₂ (μ -N ₂)} {Na(THF) ₆ } ^m	1.183(2)	1.171(4)	
(SiP ^{Ph} ₃)FeN ₂ ⁿ	1.819(2)	1.106(3)	2041
Fe(N ₂)(CO) ₂ (PEt ₃) ₂ ^o	1.853(22)	1.08(3)	2098
{Fe(PEt ₃) ₂ (CO) ₂ } ₂ (μ -N ₂) ^p	1.879(16)	1.13(2)	
{Fe(P(OMe) ₃) ₂ (CO) ₂ } ₂ (μ -N ₂) ^p	1.876(9)	1.13(1)	
{ <i>nacnac</i> Fe} ₂ (μ -N ₂) ^q	1.775(5) ^d	1.182(5)	1778
{ <i>nacnac</i> Fe} ₂ (μ -N ₂)K ₂ ^q	1.764(6) ^d	1.233(6)	1589

^a L = 2,6-[2,6-(ⁱPr)₂PhN=C(CH₃)₂(C₅H₃N)]₂(C₅H₃N); dmpc = Me₂PC₂H₄PMe₂; depe = Et₂PC₂H₄PEt₂; dippe = ⁱPr₂PC₂H₄PⁱPr₂; NP₃ = N(CH₂CH₂PPh₂)₃; CNC = 2,6-bis(aryl-imidazol-2-ylidene)pyridine (aryl = 2,6-ⁱPrC₆H₃); P₄ = Ph₂PC₂H₄PPhC₂H₄PPhC₂H₄PPh₂; PhBP^{Pr}₃ = [PhB(CH₂)P^{Pr}₃]⁻; SiP^{Ph}₃ = [(2-Ph₂PC₆H₄)₃Si]⁻; *nacnac* = β -diketiminate. ^b Ref 8. ^c Refs 5a,c. ^d Averaged values; IR stretching frequencies reported above were measured in either solid state or solution, and therefore any comparison should be taken with the appropriate precaution. ^e Refs 5b,f. ^f Ref 5d. ^g Ref 5e. ^h Ref 5g. ⁱ Ref 5j. ^j Ref 5k. ^k Ref 5l. ^l Ref 7a. ^m Ref 7c. ⁿ Ref 7b. ^o Ref 5i. ^p Ref 5h. ^q Ref 6.

Scheme 3

complexes {2-[2,6-(ⁱPr)₂PhN=C(CH₃)₂]-6-[2,6-(ⁱPr)₂PhN=C=CH₂](C₅H₃N)}Fe(μ -N₂)Na(Et₂O)₃ (**2**) and {2,6-[2,6-(ⁱPr)₂PhN=C(CH₃)₂(C₅H₃N)]₂(C₅H₃N)}Fe(μ -N₂)Na[Na(THF)₂] (**3**) isolated from the same reaction mixture via fractional crystallization from ether and THF/hexane, respectively (Scheme 3). The room-temperature magnetic moments of both complexes indicate a scenario similar to that described above for **1**. Complex **3** could also be prepared by reduction of the FeCl₂ complex with metallic sodium.

Complex **2**, the major product (Figure 2), displays features similar to complex **1**, consisting of an Fe center bound to the ligand system and to a dinitrogen unit. A Na counterion completes the structure. However, in the case of complex **2**, the Na ion is found η^1 -coordinated to the end-on, bridging dinitrogen unit forming a linear Fe–N–N–Na array. The ligand system again appears to have been deprotonated at one of the imine methyl groups. The N–N distance is longer than in **1**, 1.154(6) Å, and the Fe–N bond length has been

further shortened to 1.733(5) Å. However, the N–N stretching appears at 1965 cm⁻¹ in the IR spectrum, a frequency only slightly higher than that in **1**. The comparable bond lengths within the ligand suggest a scenario similar to complex **1**, involving a higher-valent Fe center bound to a monodeprotonated and reduced form of the ligand. The N–N distance of the dinitrogen unit may be an artifact of the different bonding modes of Na, which in turn can be ascribed to a different degree of solvation of the alkali metal.

The structure of complex **3** (Figure 3) bears resemblance to complex **1**, also consisting of an Fe center surrounded by the ligand system and an end-on coordinated molecule of dinitrogen, in turn side-on bonded to a Na atom. The presence of a second Na atom, solvated by two molecules of THF and η^3 -bound to the pyridine ring of the ligand, provides the major visible difference with complex **1**. Also, the values of the C_{imine}–C_{methyl} bond distances imply that the methyl groups in this case have not been deprotonated during the reduction. Regardless of how we consider the metal oxidation state, the formation of **3** is the result of a four-electron reduction. From the formal point of view, since the ligand displays no particularly visible modifications, and given the presence of the two Na atoms, the complex might be regarded as containing Fe in the negative divalent state. Similar to the previous cases, however, the square planar coordination geometry of the Fe atom diagnoses a more realistic, higher oxidation state. The N–N bond distance [N(4)–N(5) = 1.149(6) Å] is similar to that in **2** and is paralleled by a decrease in the Fe–N bond length and a remarkable shift of the IR stretching frequency to 1899 cm⁻¹. All of this suggests a larger extent of reduction, which, however, results in only a modest increase in N₂ activation. This again underlines the ability of the bis(iminopyridine) ligand to act as a sort of “electronic buffer” by being the preferred target of reduction. This behavior is not unprecedented in Fe chemistry, given that further reduction of an Fe–*nacnac* dinitrogen complex resulted in only a minor extent of N₂ activation, at least judging from the N–N distance.⁶

Increasing the amount of reducing agent (up to 12 equiv of NaH), allowed the isolation of two new paramagnetic species {2-[2,6-(*i*Pr)₂PhN=C(CH₃)]-6-[2,6-(*i*Pr)₂PhN–C=CH₂](C₅H₃N)}Fe–N₂ (**4**) and [{2,6-[2,6-(*i*Pr)₂PhN=C(CH₃)]₂-(C₅H₃N)}Fe–N₂]₂(μ -Na)[Na(THF)₂]₂ (**5**) which can be separated by fractional crystallization (Scheme 3). X-ray diffraction of the crystals revealed the structures displayed in Figures 4 and 5, respectively. Although the combined yield of both complexes appears to be rather low, we found no evidence in the IR spectrum of the dry reaction mixture residue for the presence of other dinitrogen complexes.

At first glance, complex **4** appears to be very similar to the species proposed by Bart et al. as generated from the double-dinitrogen complex through a dissociation equilibrium (Scheme 1).⁸ However, the C_{Me}–C_{imine} distances suggest for the present case a scenario very similar to **1** and **2** with one of the two former Me groups having been deprotonated and forming a C=CH₂ unit disordered over the two positions. The dinitrogen bond distance (N–N = 1.136 Å) and IR stretching frequency (2159 cm⁻¹, also substantially different

from that of the Bart et al.’s single dinitrogen complex⁸) reflect a small degree of reduction compared to free dinitrogen, while the Fe–N distance (1.761 Å) indicates the presence of back-bonding.

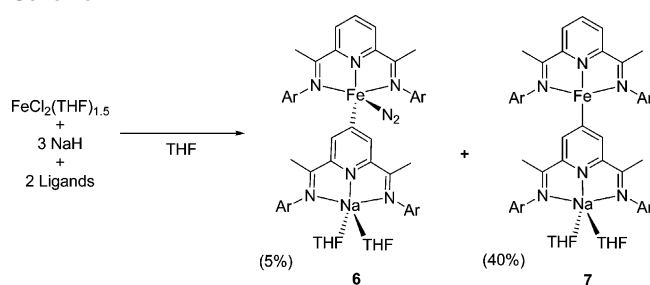
The dinuclear structure of **5** may be regarded, from the formal point of view, as resulting from the additional one-electron reduction of **3**, and further coordination to a LFeN₂ unit similar to **4**, only with intact C_{Me}–C_{imine} units. The interaction of the Na cation with the aromatic ring of the first unit and the pyridine ring of the second one is responsible for assembling the dinuclear structure. This is similar to the *intermolecular* interaction observed in the solid-state structure of **3**. The two additional Na atoms present in the molecule of **5** are π -bound to each side of the delocalized ligand backbone of the first LFeN₂ unit in an approximately η^4 fashion. Although the bridging N–N bond distance [N–N = 1.163(8) Å] is the longest among the complexes reported in this work, it is still relatively short and hard to reconcile with a two-electron reduction. However, the observed N–N stretching frequency of 1868 cm⁻¹ displays the lowest value of all dinitrogen complexes reported herein. Accordingly, the Fe–N bond length is indeed very short [Fe(1)–N(4) = 1.716(7) Å] and clearly suggestive of substantial Fe–N multiple bond character. The terminal dinitrogen moiety on the second Fe center is clearly less reduced than the first [N(9)–N(10) = 1.112(9) Å; ν = 1910 cm⁻¹].

During the isolation of complex **1** from the reaction mixture, small amounts of another complex could occasionally be crystallized from hexane. Unfortunately, the crystals were small and diffracted weakly, but in one case sufficient data were collected to enable structural determination (Figure 6). The formulation of this new paramagnetic species as {2,6-[2,6-(*i*Pr)₂PhN=C(CH₃)]₂(C₅H₃N)}Fe(η^1 -N₂)[{2,6-[2,6-(*i*Pr)₂PhN=C(CH₃)]₂(NC₅H₂)}Na(THF)₂] (**6**) was yielded by crystal structure determination revealing the presence of two ligands per Fe atom. With this information in hand, it was possible to rationally prepare **6** by performing reduction in the presence of one additional equivalent of free ligand. The yield, however, remained very low due to the presence of a second major product in the reaction mixture (see below).

The two units of **6** are connected through a σ -bond from Fe to the para-C of the pyridine ring of the Na-bound ligand displaying intact C_{Me}–C_{imine} groups. Therefore, it is tempting to speculate that one H atom has been shifted from the pyridine ring para position to one of the deprotonated C_{Me}–C_{imine} groups. In fact, the formation and orientation of the Fe–C σ -bond implies deprotonation of the para position of the pyridine ring, evidently forming a monoanionic ligand. The end-on dinitrogen unit displays a short N–N distance [N–N = 1.133(6) Å], typical of a small extent of activation of the triple bond (ν = 2009 cm⁻¹). The presence of the Na cation implies a zero-valent *formal* oxidation state for the Fe center. All other structural features of the complex are very similar to those of the other complexes described here and suggest a similar electronic configuration in spite of the clearly different *formal* oxidation states.

Formation of a complex containing two ligand systems per Fe center suggests the possibility of either ligand

Scheme 4



dissociation in solution or alternatively transmetalation of the ligand to Na. It should be reiterated from this point of view that “free” ligand, either deliberately added or generated upon dissociation from the divalent FeCl_2 precursor, does not react with NaH under the reaction conditions employed in this work. In addition, the formation of **6** requires 3 equiv of NaH per Fe (assuming 2 equiv act as reducing agents for the Fe-centered ligand and 1 equiv to deprotonate the second ligand in the para position). As mentioned above, when the preparation of complex **6** was carried out with 1 equiv of the $\text{FeCl}_2(\text{THF})_{1.5}$ starting material, 2 equiv of ligand and 3 equiv of NaH a second product was obtained in substantially larger yield upon crystallization at room temperature, or from ether. The new complex appears to be similar to **6** except for the absence of the dinitrogen unit (Scheme 4). X-ray diffraction and elemental analysis yielded the formulation of **7** as $\{2,6\text{-}[\{2,6\text{-}(\text{Pr})_2\text{PhN}=\text{C}(\text{CH}_3)_2(\text{C}_5\text{H}_3\text{N})\}\text{Fe}\{2,6\text{-}[\{2,6\text{-}(\text{Pr})_2\text{PhN}=\text{C}(\text{CH}_3)_2(\text{NC}_5\text{H}_2)\}\text{Na}(\text{THF})_2\}]\}$.

Complex **7** (Figure 7) appears to result from the dissociation of N_2 from **6**. The formation of **6** and **7** involves reduction of one ligand by two electrons and deprotonation of a second ligand at the para position of the pyridine ring to enable the formation of the $\text{Fe}-\text{C}_{\text{para}}$ attachment. The reactions leading to **6** and **7** therefore appear to be related, and a reasonable pathway in the formation of **6** may involve the fixation of dinitrogen by **7** through association–dissociation equilibrium.

At first glance, the observations reported above seem to yield a rather chaotic picture of diversified complexes having unpredictable structures and whose only common trends is the coordination of N_2 with minimal extent of reduction. However, a more careful analysis clearly shows that all of these species may in fact be related as part of the same complex behavior. Complexes **1–4** are clearly generated by a different extent of reduction, the only difference between **1** and **2** being the degree of solvation of the alkali cation and consequent different ligation mode to dinitrogen. Complex **3** may be regarded as the result of the formal addition of NaH to **1**. Complex **5** may be considered as the result of the aggregation of **3** with **4**, provided that one additional hydrogen atom may be obtained. There are several different sources for this, given the apparent mobility of the H atom of the imine Me groups as well as of the pyridine ring para position. Of course the reductant itself (NaH) may be a possible source during the Fe reduction process as part of a multimetallic redox mechanism. In fact, it is tempting to speculate that the mechanism of Fe reduction might initially proceed via the formation of intermediate $\text{Fe}-\text{H}$, where the

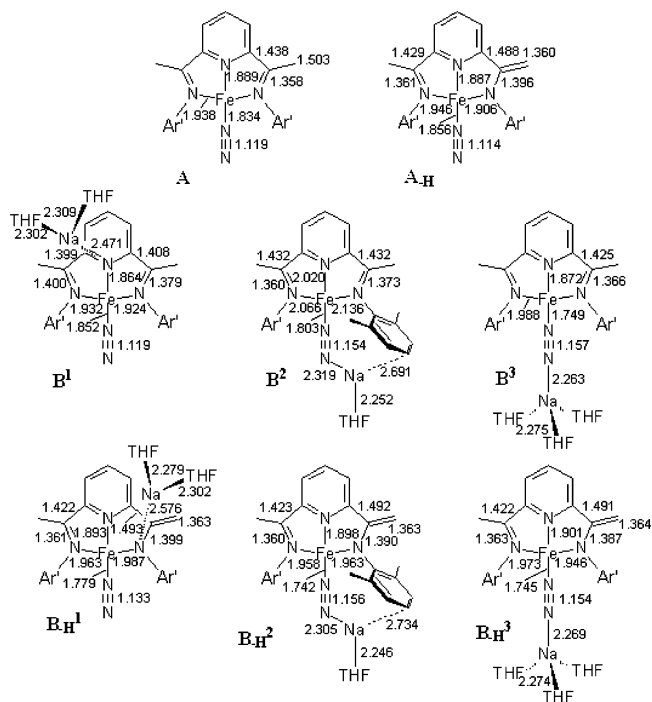


Figure 8. Calculated bond lengths (angstroms) for $\text{LFe}(\text{N}_2)$, $(\text{L}-\text{H})\text{Fe}(\text{N}_2)$, and their singly reduced derivatives ($\text{Ar}' = 2,6\text{-Me}_2\text{C}_6\text{H}_3$).

hydride subsequently performs a radical H atom abstraction from the Me group of a second unit. This would nicely explain why the formation of complex **4**, which appears to be the least reduced complex, in fact requires such a large excess of reductant. Hydrogen abstraction from the pyridine ring will instead lead to **7** and, after coordination of N_2 , to **6**. In an attempt to shed some light on this complicated behavior, we have performed density functional theory (DFT) calculations.

Bonding in $\text{LFe}(\text{N}_2)$, $(\text{L}-\text{H})\text{Fe}(\text{N}_2)$, and Reduced Derivatives. From the reactions described above, it is clear that the complexes $\text{LFe}(\text{N}_2)$ and $(\text{L}-\text{H})\text{Fe}(\text{N}_2)$ [$\text{L} = 2,6\text{-}[\{2,6\text{-}(\text{Me})_2\text{C}_6\text{H}_3\text{N}=\text{C}(\text{CH}_3)_2(\text{C}_5\text{H}_3\text{N})\}\text{Fe}\{2,6\text{-}[\{2,6\text{-}(\text{Me})_2\text{C}_6\text{H}_3\text{N}=\text{C}(\text{CH}_3)_2\}\text{C}(\text{CH}_3)_2(\text{C}_5\text{H}_3\text{N})\}\text{Na}(\text{THF})_x\}]\}$] can accept several electrons and that the counterions $\text{Na}(\text{THF})_x^+$ can bind to the reduced species in various ways: to the terminal nitrogen of the N_2 ligand, to an imine arene group, or to the diiminepyridine ligand π -system. This ease of reduction is remarkable, since $\text{LFe}(\text{N}_2)$ already contains a two-electron-reduced ligand, i.e., it should be described as $(\text{L}^{\cdot-})\text{Fe}^{\text{II}}(\text{N}_2)$. Several questions arise: Where do the electrons go, to the metal or to the ligand? To what extent does the N_2 ligand get reduced (“activated”) in this process? Are there any significant differences between the reduction of $\text{LFe}(\text{N}_2)$ and $(\text{L}-\text{H})\text{Fe}(\text{N}_2)$? The location of hydrogen atoms in X-ray structures is always difficult, so for several complexes described in this work there is some uncertainty about possible deprotonation of an imine methyl group. Can bond lengths within the ligand help to decide between $\text{LFe}(\text{N}_2)$ and $(\text{L}-\text{H})\text{Fe}(\text{N}_2)$ complexes? We have addressed these issues using DFT calculations. For reasons of computational efficiency, the bulky $2,6\text{-}i\text{Pr}_2\text{C}_6\text{H}_3$ groups have been replaced by slightly less bulky $2,6\text{-Me}_2\text{C}_6\text{H}_3$ groups. Figures 8–10 show the structures studied, with relevant bond lengths. A

Reduction of an Fe Bis(iminopyridine) Complex

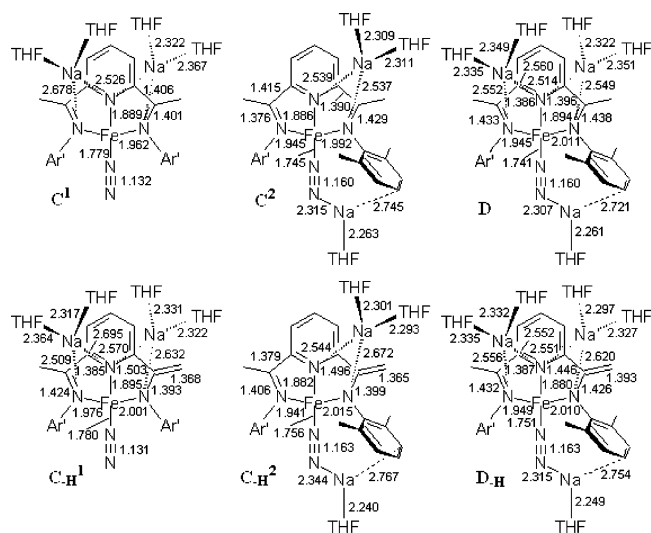


Figure 9. Calculated bond lengths (angstroms) for doubly (**C**) and triply (**D**) reduced derivatives.

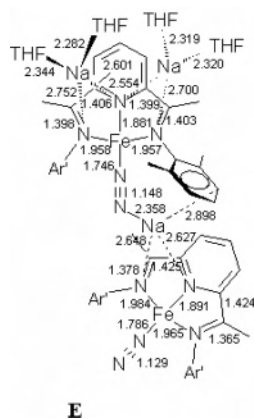


Figure 10. Calculated bond lengths (angstroms) for model **E** for complex **5**.

variety of spin states (at least up to four or five unpaired electrons) have been considered for model complexes (i.e., without bulky aryl groups). In all cases where the formal oxidation state of Fe was zero or lower, the lowest spin state always was the lowest in energy. For calculations on the “real” systems (i.e., with 2,6-Me₂C₆H₃ instead of 2,6-ⁱPr₂C₆H₃), the geometries of the lowest spin state ($S = 0$ or $1/2$) and the next-highest one ($S = 1$ or $3/2$) have been optimized for all systems. Again, the lowest spin state was consistently yielding the lowest energy.

Bonding of N₂ to LFe and (L–H)Fe. Calculations predict very similar N₂ binding energies for LFe and (L–H)Fe (ca. 19 and ca. 17 kcal/mol to form complexes **A** and **A**_H, respectively). Also, the geometries of the resulting Fe(N₂) moieties are very similar (Fe–N = 1.834 Å and 1.856 Å; N≡N = 1.119 Å and 1.114 Å, vs 1.101 Å in free N₂ at the same level). Inspection of occupied orbitals and of bond lengths within the ligands indicates significant additional electron transfer from metal to ligand in both cases. As anticipated, the complexes are best formulated as containing Fe^{II} and either L^{•+} or (L–H)[•]. Apparently, the ligand effects of L^{•+} and (L–H)[•] are rather similar [in earlier work on binuclear vanadium complexes, we have noted the similarity between L^{•+} and (L–2H)²⁻].¹³ The calculated Fe–N dis-

tances are uniformly larger than the observed ones (by ca. 0.1 Å). This seems to be a systematic failure of this type of DFT calculation. The elongation of the N≡N bond on complexation to either LFe or (L–H)Fe is modest (ca 0.015 Å) and points to a very limited amount of back-donation from Fe to N₂.

One-Electron Reduction. For both **A** and **A**_H, we considered three possible reduction products each (**B**¹–**B**³ and **B**¹_H–**B**³_H): (1) A Na(THF)₂ unit coordinated to the ligand π -system; (2) A Na(THF) moiety bound to the terminal N₂ nitrogen and an imine arene group; (3) A Na(THF)₃ unit bound to the terminal N₂ nitrogen.

Relative to **A**, structure **B**¹ shows a clear elongation of the C_{im}–N_{im} bonds and corresponding shortening of C_{py}–C_{im} bonds, but very little change otherwise. In particular, the Fe–N and N≡N distances hardly change. This indicates that the extra electron has gone to a ligand π^* orbital. Similar reduction of **A**_H results in a structure with Na close to the amide nitrogen. Now, the bond lengths in the imine “arm” of the ligand do not change, but the Fe–N_{amide} bond gets longer (by 0.08 Å) as does N≡N (by 0.02 Å), while the Fe–N₂ distance *decreases* by 0.07 Å. All of this indicates that reduction has happened at the Fe atom and has resulted in increased back-donation to the N₂ unit. Metal-centered reduction is also indicated for structures **B**²–**B**³ and **B**²_H–**B**³_H; the main difference with **B**¹_H is that for these bridged structures the N≡N is more elongated, by up to 0.05 Å.

From these results, we can draw the following conclusions. (1) The site of reduction is clearly indicated by bond length changes: reduction at the metal shortens Fe–N₂ and lengthens the Fe–N_{im} and Fe–N_{py} bonds, whereas ligand-centered reduction affects mainly the imine groups. (2) LFe(N₂) can more easily accept electrons into its ligand π -system than (L–H)Fe(N₂). (3) The location of the Na(THF)_x⁺ counterion can be important in directing the site of reduction of LFe(N₂). Coordination to the π -system stabilizes the π^* orbitals and therefore promotes ligand-centered reduction, whereas coordination to N₂ favors metal-centered reduction and back-donation to N₂.

If we now compare the X-ray structure of complex **4** with those of complexes **1** and **2**, we see increases in the Fe–N_{im} and Fe–N_{py} bond lengths, shorter Fe–N₂ bonds, and virtually unchanged ligand imine groups. This agrees with the calculations and indicates metal-centered reduction. The curiously short N≡N bond observed for complex **1** is not reproduced in the calculated structures of *any* singly reduced structure containing either L or (L–H), and we conclude that it is most likely an artifact. It should be noted here that the observed changes in N≡N bond lengths are relatively small (at most 0.05 Å) compared to the errors of X-ray structure determinations and should therefore be treated with caution (a similar observation was made recently for C–O bond lengths in a large series of metal carbonyl complexes³¹ was relatively poor as noted earlier.

In the X-ray structure of complex **4** [LFeN₂], the C_{im}–C_{Me} bond length of 1.454 Å is short for a terminal C_{im}–CH₃ bond (calculated, 1.503 Å) and could in principle represent a deprotonated C_{im}=CH₂ group disordered over

two positions (calculated, 1.432 Å).³⁰ As a word of caution, it should be noted here that abnormally short terminal C_{im}–CH₃ bonds have been observed in other cases where clearly no deprotonation has taken place.³¹ This seems to be an artifact, since calculations produce very constant C_{im}–CH₃ bond lengths. We tentatively conclude that terminal C_{im}–CH₃ bond lengths in the range of ca. 1.43–1.47 Å from X-ray structure determinations are not very reliable indicators of the deprotonation state of the ligand. The average C_{im}–N_{im} and C_{py}–C_{im} bond lengths observed for complex **4** (1.362 and 1.434 Å) are very close to the values calculated for **A**; agreement with **A**–H (1.379 and 1.459 Å) is somewhat poorer. Some uncertainty remains in the assignment of the deprotonation state of complex **4**.

Similar to complex **4**, the observed bond lengths for complexes **1** and **2** do not allow a completely unambiguous assignment of the ligand protonation state, although in this case the agreement is slightly better for the deprotonated structure.

Further Reduction. Two-electron reduction of **A** (to give **C**¹ or **C**², see Figure 9) results in the transfer of one electron to the ligand and one to the metal center so that the final product should be formulated as having Fe^I regardless of the location of the Na counterions. It appears that the diiminepyridine ligand, having already accepted two electrons in the π* system in **A** and one more upon one-electron reduction to **B**¹, is reluctant to accept a fourth π* electron. This is consistent with our earlier observation of up to three-electron reduction of L by metallic lithium.¹⁷ Any four-electron-reduced structure would necessarily have at least one negative charge on a carbon not bound to Fe, which we assume to be an unfavorable situation.

Two-electron reduction of **A**–H also results in transfer of one electron to the metal and one to the ligand, regardless of the Na positions. The ligand is now fully trianionic, with a full negative charge on each nitrogen atom.

Turning to the X-ray structure of complex **3**, we see that again the intraligand bond lengths would be compatible with either **C**² or **C**²–H. The terminal C_{im}–C_{Me} bond lengths observed in the X-ray structure, however, are such that formulation of a nondeprotonated complex seems more reasonable.

In the triply reduced species **D**, we see that the ligand π* orbitals have finally absorbed a fourth electron. The deformation of the imine groups is extreme, whereas the Fe–N₂ unit is very similar to that in **C**².

The last structure we considered is **E** (Figure 10) as a model for “dimeric” complex **5**. Calculated bond lengths within the LFe(N₂) unit bound to all three Na atoms are very similar to those in **C**¹ and indicate that ligand and metal have

Table 4. Comparison of Reduction of **A** and **A**–H

entry	reaction (see Figures 8 and 9)	ΔE (kcal/mol)
1	B ² + B ¹ → C ² + A	–3.4
2	B ¹ + B ¹ → C ¹ + A	–9.1
3	C ¹ + B ² → D + A	1.9
4	2 B ² + B ¹ → E + A	–29.2
5	B – ² _H + B – ¹ _H → C – ² _H + A –H	+7.2
6	B – ¹ _H + B – ¹ _H → C – ¹ _H + A	+5.6
7	C – ¹ _H + B – ² _H → D –H + A –H	+22.7
8	B ¹ + A –H → B ¹ –H + A	–10.4
9	B ² + A –H → B ² –H + A	0.3
10	B ³ + A –H → B ³ –H + A	–4.9
11	C ¹ + A –H → C ¹ –H + A	0.5
12	C ² + A –H → C ² –H + A	–0.5
13	D + A –H → D –H + A	+9.7

each accepted one electron (relative to **A**). This implies that one electron must have transferred to the second LFe(N₂) unit. Interestingly, bond lengths within this second unit indicate that, different from **B**¹, the electron has reduced the metal rather than the ligand. The reason for this difference is not clear at present. Apparently, the ligand-reduced and metal-reduced variations of LFe(N₂) are very close in energy, and small changes in the complex can tip the balance either way. This fluidity also means that in solution metal-reduced and ligand-reduced species could be in fast equilibrium.

The C_{im}–C_{Me} bond lengths of complex **5** indicate that no ligand deprotonation has occurred. Comparison of bond lengths with those calculated for **E** shows reasonable agreement, although differences in particular for the imine groups are larger than in the other complexes. Nevertheless, it seems safe to conclude that in complex **5** one LFe(N₂) unit is doubly reduced (at metal and ligand) and one is singly reduced (at metal only).

Energetics of Reduction. Table 4 lists the energies associated with successive reduction steps of the Fe complexes. Here, we see an interesting difference between the deprotonated and nondeprotonated systems. For the deprotonated complexes, the second reduction step (**B** → **C**, entries 5 and 6) is more difficult than the first, and the third one (entry 7) is harder still, as one might intuitively expect. For the nondeprotonated systems, however, the second reduction is predicted to be easier than the first (entries 1 and 2), and even the third is not much more difficult (entry 3). When both series are compared, it becomes clear that in particular the first reduction step is more difficult for **A** than for **A**–H (entries 8 and 10). Thus, the nondeprotonated series is predicted to have a preference for forming more reduced species, to the extent that the disproportionation reaction 3 **B** → **E** + **A** is calculated to be strongly exothermic (entry 4).

Calculated energies for species of different multiplicities, as reported here, need to be treated with caution. Also, the present system seems to be rather complex, with a subtle balance between kinetics, thermodynamics and ease of crystallization leading to the various products isolated. However, the above results seem to agree with the observation that the monodeprotonated species are mainly found in singly reduced states, whereas the more strongly reduced species appear not to be deprotonated.

(30) A localized deprotonated (L–H)Fe(N₂) structure is clearly incompatible with the observed bond lengths.

(31) See, e.g., (a) Hiya, K.; Nakayama, Y.; Yasuda, H. *Macromolecules* **2003**, *36*, 7916. (b) Unni Nair, B. C.; Sheats, J. E.; Ponteciello, R.; Van Engen, D.; Petrouleas, V.; Dismukes, G. C. *Inorg. Chem.* **1989**, *28*, 1582. (c) Chen, Y.; Chen, R.; Qian, C.; Dong, X.; Sun, J. *Organometallics* **2003**, *22*, 4312. (d) Vasilevsky, I.; Rose, N. J.; Stenkamp, R. E. *Acta Crystallogr.* **1992**, *B48*, 444. (e) Small, B. L.; Brookhart, M.; Bennett, A. M. *J. Am. Chem. Soc.* **1998**, *120*, 4049. (f) Brooker, S.; McKee, V. *Chem. Commun.* **1989**, 619.

Conclusion

Reduction of LFeCl_2 , or of a mixture of L and FeCl_2 , is a complex reaction, forming a slew of Fe–dinitrogen products, presumably even more than we have isolated up until now. Reduction to formally zero-valent Fe complexes has been reported before, but our results demonstrate that further reduction (up to formally Fe^{2-}) is possible. Thus, the diiminepyridine ligand is comparable to a set of carbon monoxide ligands in stabilizing very low metal oxidation states [cf., $\text{Fe}(\text{CO})_4^{2-}$]. It appears that, starting from $\text{LFe}(\text{N}_2)$ (which already has two electrons in ligand π^* orbitals) at most one additional electron goes to the ligand system. Further reduction occurs at the metal center and increases back-donation to the N_2 ligand. $(\text{L}-\text{H})\text{Fe}(\text{N}_2)$ is really $(\text{L}-\text{H})^{\bullet} \text{Fe}^{\text{II}}(\text{N}_2)$, and reduction occurs first at the metal and then at the ligand. In the unusual “dimeric” complex **5**, one unit has been reduced at the metal and the ligand and the other unit has been reduced at the metal only.

The $\text{LFe}(\text{N}_2)$ and $(\text{L}-\text{H})\text{Fe}(\text{N}_2)$ fragments are very similar in their Fe– N_2 interaction and reduction behavior. Averaged bond lengths for $\text{L}^{\bullet} \text{Fe}$ and $(\text{L}-\text{H})^{\bullet} \text{Fe}$ (or any of their reduced versions) are also very similar in most cases. On the one hand, this makes it difficult to distinguish between complexes containing intact and deprotonated ligands on the basis of bond lengths. On the other hand, the similar behavior of the two fragments means that distinguishing them may not always be that important.

It is interesting to note that fixation of dinitrogen by late transition metal bis(iminopyridine) systems (Fe^8 and $\text{Co}^{20,21}$) results in weakly activated and mainly terminal, end-on dinitrogen units, whereas dinitrogen complexes of V^{13} and Cr^{15} bis(iminopyridine) systems adopt bimetallic structures with end-on N_2 bridges. The immobilization of the dinitrogen unit between the two metal centers allows for a greater degree of reduction of the triple bond. In fact, the $\text{V}-\text{N}_2$ unit undergoes a two-electron reduction and the $\text{Cr}-\text{N}_2$ unit may accept six electrons and result in complete cleavage of the triple bond.¹⁵ The ideal situation for N_2 activation therefore appears to involve a bimetallic attack of the associated dinitrogen moiety, an outcome that is not easy to attain with late metal systems.

Acknowledgment. This work was supported by NSERC and the Canada Foundation for Innovation (CFI project 10831) and the Manitoba Research and Innovation Fund. Use of computer resources from WestGrid (www.westgrid.ca) by P.H.M.B. is gratefully acknowledged.

Supporting Information Available: Tabulated total energies and S^2 expectation values for model complexes **A–E**, PDF files for all calculated structures, complete crystallographic data (as a CIF file) for complexes **1–7**. This material is available free of charge via the Internet at <http://pubs.acs.org>.

IC701643D